0888-8809/04/$15.00/0
Printed in U.S.A.

Molecular Endocrinology 18(8):1887–1905

doi: 10.1210/me.2003-0334

Molecular Mechanism for the Potentiation of the Transcriptional Activity of Human Liver Receptor Homolog 1 by Steroid Receptor Coactivator-1

PING-LONG XU, YUN-QING LIU, SHI-FANG SHAN, YU-YING KONG, QING ZHOU, MEI LI, JIAN-PING DING, YOU-HUA XIE, AND YUAN WANG

State Key Laboratory of Molecular Biology (P.-L.X., S.-F.S., Y.-Y.K., Q.Z., M.L., Y.-H.X., Y.W.) and Key Laboratory of Proteomics (Y.-Q.L., J.-P.D.), Institute of Biochemistry and Cell Biology, Shanghai Institutes for Biological Sciences, Chinese Academy of Sciences, Shanghai 200031, China

The liver receptor homolog 1 (LRH-1) belongs to the *Fushi tarazu* factor 1 nuclear receptor subfamily, and its biological functions are just being unveiled. The molecular mechanism for the transcriptional regulation by LRH-1 is not clear yet. In this report, we use mutagenesis and reporter gene assays to carry out a detailed analysis on the hinge region and the proximal ligand binding domain (LBD) of human (h) LRH-1 that possess important regulatory functions. Our results indicate that helix 1 of the LBD is essential for the activity of hLRH-1 and that the steroid receptor coactivator (SRC)-1 interacts directly with the LBD of hLRH-1 and significantly potentiates the transcriptional activity of hLRH-1. Cotransfection assays demonstrate that overexpressed SRC-1 potentiates hLRH-1 mediated activation of the cholesterol 7-α-hydroxylase promoter and increases the transcription of the endogenous cholesterol 7-α-hydroxylase in Huh7 cells. The interaction between SRC-1 and hLRH-1 assumes a unique pattern that involves primarily a region containing the glutamine-rich domain of SRC-1, and helix 1 and activation function-2 of hLRH-1 LBD. Mutagenesis and molecular modeling studies indicate that, similar to mouse LRH-1, the coactivator-binding cleft of hLRH-1 LBD is not optimized. An interaction between helix 1 of hLRH-1 LBD and a region containing the glutamine-rich domain of SRC-1 can provide an additional stabilizing force and enhances the recruitment of SRC-1. Similar interaction is observed between hLRH-1 and SRC-2/transcriptional intermediary factor 2 or SRC-3/acetyltransferase. Moreover, transcriptional intermediary factor 2 and acetyltransferase also potentiate the transcriptional activity of hLRH-1, suggesting a functional redundancy among SRC family members. These findings collectively demonstrate an important functional role of helix 1 in cofactor recruitment and reveal a novel molecular mechanism of transcriptional regulation and cofactor recruitment mediated by hLRH-1. (*Molecular Endocrinology* 18: 1887–1905, 2004)

THE LIVER RECEPTOR homolog 1 (LRH-1) is a member of the *Fushi tarazu* factor 1 (FTZ-F1) orphan nuclear receptor (NR) family that also includes the steroidogenic factor 1 (SF-1) (1). Like other NRs, LRH-1 is composed of several modular functional domains, including an N-terminal A/B domain, a characteristic zinc finger DNA binding domain (DBD), a hinge region, and a C-terminal ligand binding domain (LBD). FTZ-F1 related receptors also contain a special FTZ-F1 box that is located at downstream from the zinc fingers and bind to the target site as monomer (Fig. 1A) (2). LRH-1 and SF-1 exhibit distinct yet overlapping expression patterns. SF-1 exists mainly in steroidogenic tissues as a key regulator for the development and differentiated function of the adrenal gland and gonads (3, 4). LRH-1 has been demonstrated to express in liver, pancreas, intestine, ovary, adrenal, and preadipocytes (5–8), and its biological functions are just being unveiled. LRH-1 acts as an important tissue-specific transcriptional activator in bile acid and cholesterol homeostasis by regulating several key enzymes and transporters (9–13). Among them, the cholesterol 7-α-hydroxylase (CYP7A1) gene encodes the first and rate-limiting enzyme in bile acid synthesis,

Abbreviations: aa, Amino acids; ACTR, acetyltransferase; AD, activation domain; AF-2, activation function-2 domain; ATRA, all-*trans* retinoic acid; bHLH-PAS, basic-helix-loop-helix/Per/ARNT/Sim; CBP, cAMP response element binding protein (CREB)-binding protein; CYP7A1, cholesterol 7-α-hydroxylase; DBD, DNA binding domain; ENII/Cp, enhancer II and core promoter of HBV; FTZ-F1, *Fushi tarazu* factor 1; GST, glutathione-*S*-transferase; h, human; HBV, hepatitis B virus; HNF, hepatocyte nuclear factor; KO, knockout; LRH-1, liver receptor homolog-1; LBD, ligand binding domain; NID, nuclear receptor-interacting domain; NIDm, mutant NID; NR, nuclear receptor; Q-rich, glutamine-rich; PPAR, peroxisome proliferator-activated receptor; RAR, retinoic acid receptor; RXR, retinoid X receptor; SF-1, steroidogenic factor-1; SMRT, silencing mediator of retinoic acid and thyroid hormone receptors; SRC, steroid receptor coactivator; TIF2, transcriptional intermediary factor 2.

***Molecular Endocrinology* is published monthly by The Endocrine Society (http://www.endo-society.org), the foremost professional society serving the endocrine community.**

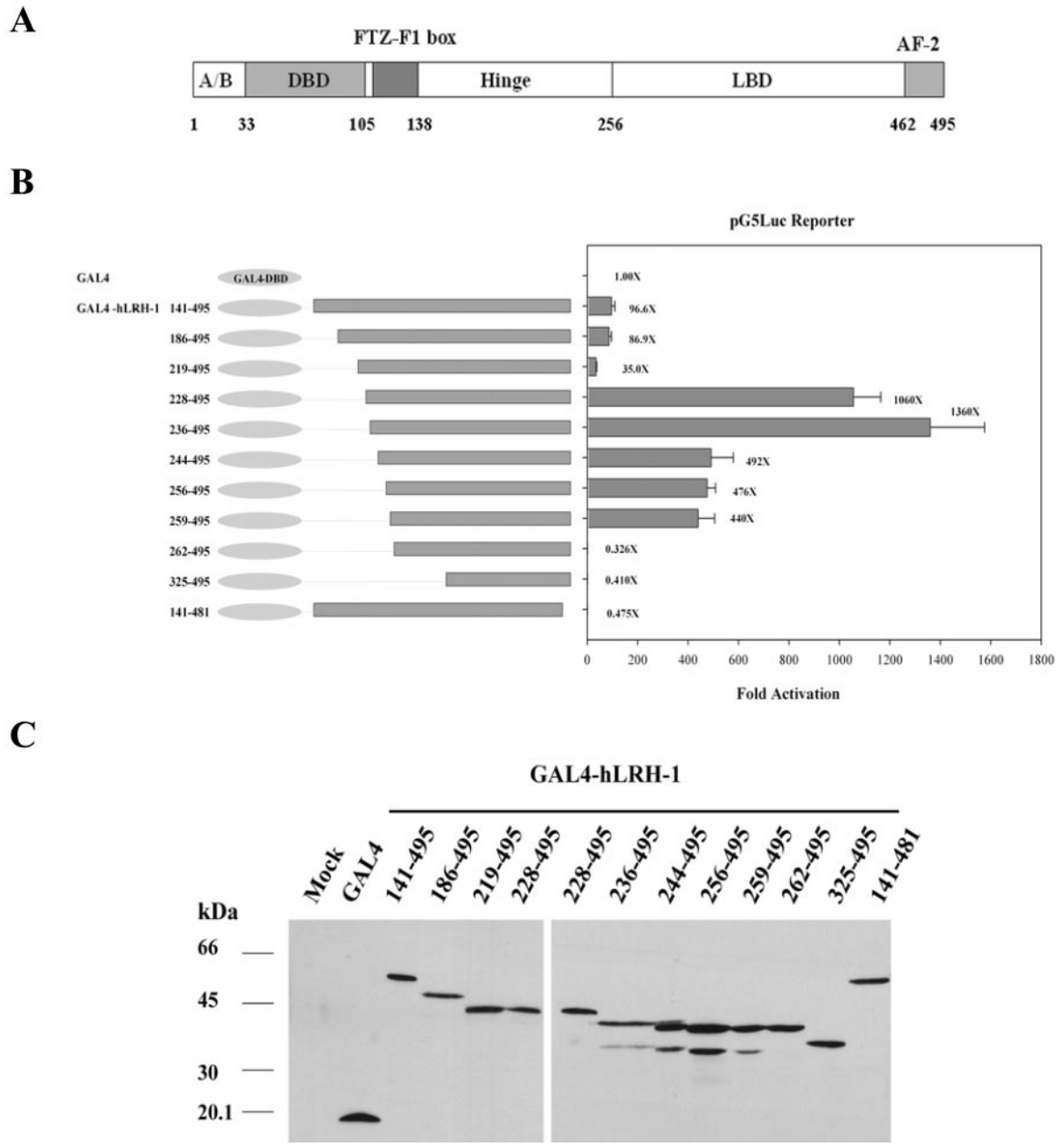

Fig. 1. Potential Functional Segments within the Hinge Region and the Proximal LBD of hLRH-1

A, Schematic representation of the modular structure of hLRH-1. B, *Left panel,* Schematic representation of 5′-deletions in the hinge region and the proximal LBD of hLRH-1 fused with GAL4-DBD. *Right panel*, Activity of each GAL4-hLRH-1 fusion protein (0.5 μg) was tested in Huh7 cells using the pG5Luc reporter (1 μg per dish) and is shown as fold activation above the basal activity (pM), which is taken as 1. The average values with SD from three independent duplicate experiments are shown. C, Expression of the GAL4-hLRH-1 fusion proteins was examined with Western blot assays.

and LRH-1 has been identified as an essential regulator for its transcription. Besides, LRH-1 can modulate the expression of aromatase (8) and several liver-enriched transcriptional factors such as hepatocyte nuclear factor (HNF)1α, HNF3β, and HNF4α (14). In addition to these cellular genes, our previous works have also shown that human (h) LRH-1 can activate hepatitis B virus enhancer II, which in turn regulates hepatic viral gene expression and replication (15, 16).

Despite accumulating biochemical and mutagenesis data on the diverse biological functions, the functional domains of LRH-1 and the underlying molecular mechanism of the transcriptional regulation mediated by LRH-1 are not clear. It is well documented that NR-mediated transcription often requires the recruitment of specific coregulators (17). Biochemical data have shown that AF-2 and an identity box in the LBD are essential for the transcriptional activity of the zebrafish FTZ-F1 ho-

molog, zFF1 (18). SF-1 can interact with multiple coregulators (19–22) and maximal SF-1-mediated transcription and cofactor recruitment depend on the phosphorylation of Ser203 in the hinge region (23).

The p160 steroid receptor coactivator (SRC) family contains three homologous members, SRC-1 (nuclear receptor coativator-1), SRC-2 [transcriptional intermediary factor 2 (TIF2), glucocorticoid receptor-interacting protein-1, nuclear receptor coactivator-2], and SRC-3 [acetyltransferase (ACTR), p300/cBP-interacting protein, receptor-associated coactivator-3, amplified in breast cancer-1, thyroid hormone receptor activator module-1] (24–34). These coactivators interact with NRs in a ligand-dependent manner to recruit histone acetyltransferases, histone methyltransferases, coactivator-associated arginine methyltransferase 1, and protein methyltransferase-1 (35–38) to specific enhancer/promoter regions, which facilitates chromatin remodeling, assembly of general transcription factors, and transcriptional regulation of target genes. SRC-1 plays an important role in SF-1 mediated transcription. A mammalian two-hybrid assay suggests that SF-1 may interact with SRC-1 via AF-2 and a proximal element [amino acids (aa) 187–245] in the hinge region, although a direct interaction between SF-1 and SRC-1 has not been demonstrated (39, 40). These data suggest that the hinge region and other regions of the LBD in addition to AF-2 may possess important regulatory functions for the transcriptional activity of FTZ-F1-related receptors. This notion is further supported by analyzing the activities of two other hLRH-1 variants resulted from alternative splicing (11, 15). The longer variant (hB1F2) that contains 46 additional amino acids in the middle of the A/B domain is also a transcriptional activator. However, the shorter variant (CPFv2) that lacks most of the hinge region and the N-terminal part of the LBD (aa 153–324 of hLRH-1) is inert in transcriptional activation, suggesting that the hinge region and/or the proximal LBD are important for the activity of hLRH-1.

In this paper, we use mutagenesis and reporter gene assay methods to characterize the functional roles of the hinge region and the LBD of hLRH-1. We identified several structural segments in these regions that can greatly affect the transcriptional activity of hLRH-1. In particular, helix 1 of the LBD is shown to be essential for the transcriptional activity of hLRH-1. We also discovered that SRC-1 could potentiate the transcriptional activity of hLRH-1 through a direct interaction with its LBD. This interaction involves primarily a region containing the glutamine-rich domain of SRC-1, and helix 1 and AF-2 of hLRH-1. We demonstrate that overexpressed SRC-1 can potentiate hLRH-1-mediated activation of the liver-specific CYP7A1 promoter and increase the endogenous CYP7A1 transcription in Huh7 cells. Similarly, TIF2 and ACTR also interact directly with hLRH-1 and potentiate the transcriptional activity of hLRH-1. With the availability of the recently reported crystal structure of the LBD of mouse LRH-1 (mLRH-1) (41), we have built a three-dimensional homology model of hLRH-1 LBD and discuss the biochemical and mutagenesis data and the potential functional roles of these structural segments in the context of the model. These findings illustrate a unique property of LRH-1 in cofactor recruitment and demonstrate a novel interaction mode between members of the SRC family and an NR.

RESULTS

Potential Functional Segments within the Hinge Region and the Proximal LBD of hLRH-1

To identify the functional elements in the hinge region and the proximal LBD of hLRH-1, deletion analyses were performed starting from residue 141, the putative beginning of the hinge region. The deletion regions were carefully chosen based on the predicted secondary structures to avoid disruption of potential helix structures and to minimize possible misfolding effects. Each truncated hLRH-1 was fused with the C terminus of the GAL4 DBD (Fig. 1B). The transcriptional activities of these fusion proteins were examined in Huh7 cells with reporter assays. As shown in Fig. 1B, GAL4-hLRH-$1_{141–495}$ containing the complete hinge region and the LBD was fully active. Truncation to residue 219 partially impaired the activity. However, truncation to residue 228 caused a dramatic increase in the transcriptional activity, suggesting a putative strong repression element between aa 219 and 227. Further truncations to residues 244, 256, and 259 resulted in moderate decrease of activities. Because residue 256 is the putative boundary between the hinge region and the LBD, these results indicate that hLRH-1 LBD alone is active. However, truncation to residue 262 not only completely abolished the transcriptional activity but also showed a repression. Further truncation to residue 325, which is the C terminus of the internal deletion in the CPFv2 variant, displayed a similar repression. Moreover, GAL4-hLRH-$1_{141–481}$, in which activation function-2 (AF-2) was partially deleted, also lost the transcriptional activity and behaved as a repressor.

Western blot assays with the whole cell lysates were performed to examine the expression of these fusion proteins. Detected with an anti-GAL4 monoclonal antibody, the expression levels of all fusion proteins are comparable (Fig. 1C). Therefore, the differences in the transcriptional activities of the fusion proteins are not likely due to the slightly varying protein expression levels or protein stability; instead, reflect an intrinsic property of hLRH-1. Although bands of lower molecular weight impurities were observed in some lanes, they should not alter the result interpretation. Collectively, the results suggest that hLRH-1 contains a structural element between aa 219 and 227 of the hinge region that can repress the transcriptional activity of hLRH-1 and a crucial structural element at the N terminus of the

LBD that plays an important role in the transcriptional activity of hLRH-1.

Helix 1 of the LBD Is Essential for the Activity of hLRH-1

The reporter assays reveal that the structural segment containing aa 259–261 at the N terminus of the LBD is crucial for the transcriptional activity of hLRH-1. Secondary structure prediction and homology modeling studies show that this segment belongs to an α-helix (aa 257–264) at the N terminus of the LBD (Figs. 2A and 3). This helix (helix 1) forms part of the conserved sandwich framework structure found in other nuclear receptors (42). The hydrophobic side of helix 1 packs with helices 8 and 9 via extensive hydrophobic interactions and its hydrophilic side is exposed to the solvent.

Mutagenesis studies were carried out to scrutinize the functional role of helix 1 (Fig. 2B). As shown in Fig. 2C, the $TSS_{251}AAA$ mutant, in which three amino acids

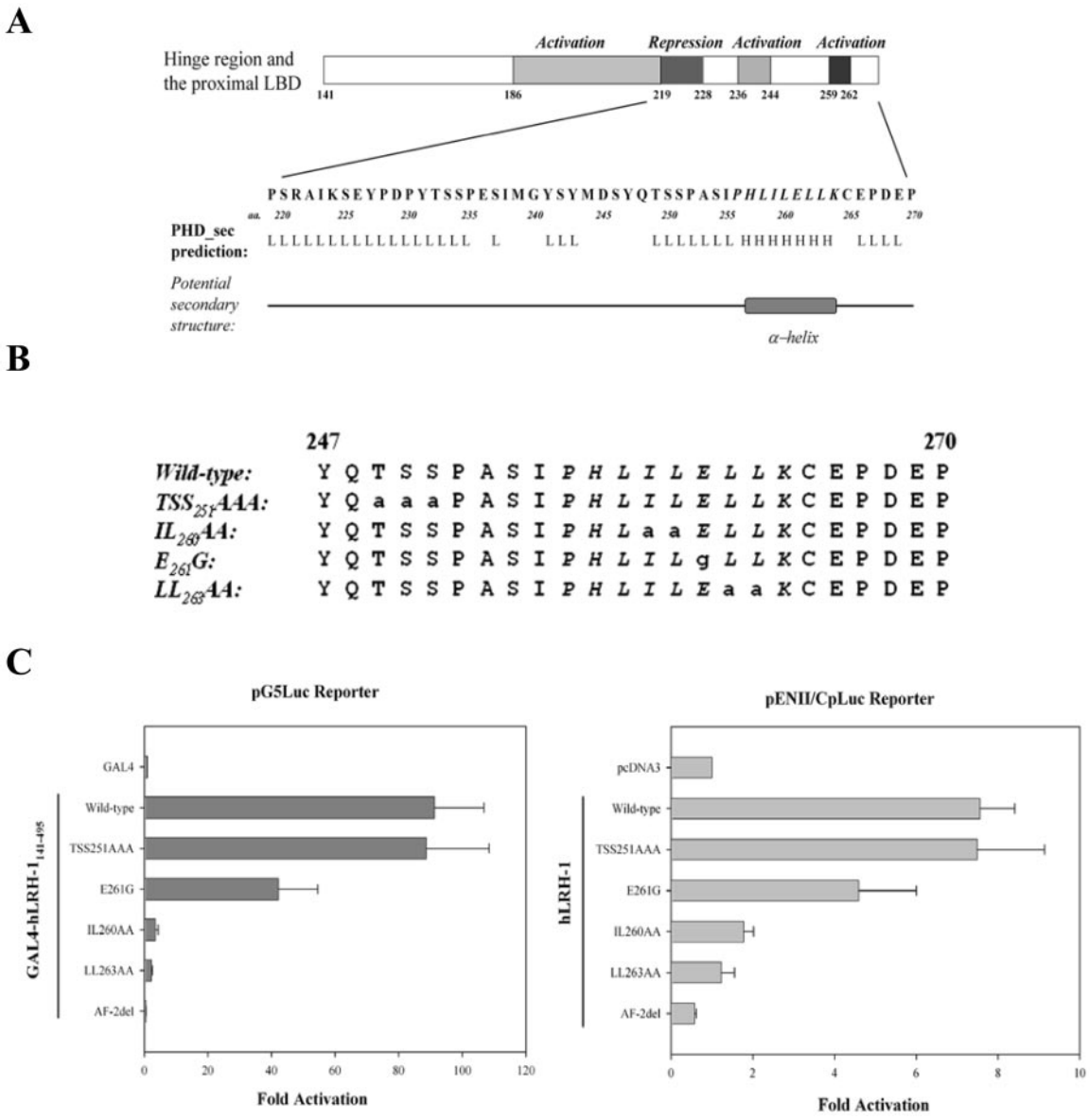

Fig. 2. Helix 1 of the LBD Is Essential for the Activity of hLRH-1

A, Helix 1 at the N-terminal of the hLRH-1 LBD as predicted by PHD_sec software. H, Helix; L, loop; *space*, no prediction (Rel $<$ 5). B, Point mutations in helix 1. The mutated residues are in *lowercase letters*. C, *Left panel*, Activity of each GAL4-hLRH-1 mutant containing point mutations in helix 1 (0.5 μg) was tested in Huh7 cells using the pG5Luc reporter or (1 μg per dish) and is shown as fold activation above the basal activity (pM), which is taken as 1. (*right panel*) Activity of each hLRH-1 helix 1 mutant (0.5 μg) was also tested in Huh7 cells using the pENII/CpLuc reporter (1 μg per dish) and is shown as fold activation above the basal activity (pcDNA3), which is taken as 1. The average values with SD from three independent duplicate experiments are shown.

($T_{249}S_{250}S_{251}$) located at the linker from the hinge region to helix 1 of the LBD were altered to alanines, retained a transcriptional activity similar to wild-type GAL4-hLRH-$1_{141–495}$. In contrast, mutations within helix 1, specifically $E_{261}G$, $IL_{260}AA$, and $LL_{263}AA$, caused moderate to dramatic decrease of activities. Similar results were obtained from the transfection experiments using a luciferase reporter driven by a natural hLRH-1-responsive promoter, the enhancer II and core promoter of hepatitis B virus (HBV ENII/Cp). In Huh7 cells, the exogenous expression of wild-type hLRH-1 (0.5 μg) activated the reporter by about 7.5-fold compared with the empty vector. The $TSS_{251}AAA$ mutant exhibited a transcriptional activity similar to wild-type hLRH-1. A moderate activation was observed with the $E_{261}G$ mutant (4.6-fold). However, the $IL_{260}AA$ mutant only activated the reporter by 1.8-fold and the $LL_{263}AA$ mutant barely showed any transcriptional activity. In both reporter gene assays, the AF-2 partial deletion mutant of hLRH-1 (AF-2del) was inert in transactivation. Taken together, the reporter assays clearly indicate that helix 1 (aa 257–264) is essential for the transcriptional activity of hLRH-1.

The functional roles of these residues and the effects of these mutations on the transcriptional activity of hLRH-1 were examined in the context of the three-dimensional model of hLRH-1 LBD (Fig. 3). Modeling studies show that I259 and L262 point their side chains inward toward the hydrophobic core and form extensive hydrophobic interactions with residues of helices 8 and 9. E261 points its side chain outward on the surface and forms a salt bridge with the positively charged side chain of K264. These two charged residues form an electrostatic patch on the LBD surface and could take part in interactions with a potential ligand or coactivator. Mutation of E261G would disrupt its interaction with K264 and is likely to affect its interaction with a ligand or coactivator. The side chains of L260 and L263 are partially exposed on the surface and form a hydrophobic patch on the protein surface. Specifically, the side chain of L260 has hydrophobic contacts with the side chain of I255 at the N terminus of LBD; the side chain of L263 has contacts with the aliphatic side chains of G399 and R400 of helix 8. Molecular dynamics simulations indicate that all of these mutations do not affect the main-chain conformation of helix 1 and the overall sandwich framework of NR structure. However, the mutations $IL_{260}AA$ or $LL_{263}AA$ could affect the hydrophobic interactions with residues of helices 8 and 9 and consequently the precise position of helix 1. Thus, these mutations would affect the interactions of hLRH-1 LBD with a ligand or coactivator and the transcriptional activity of hLRH-1.

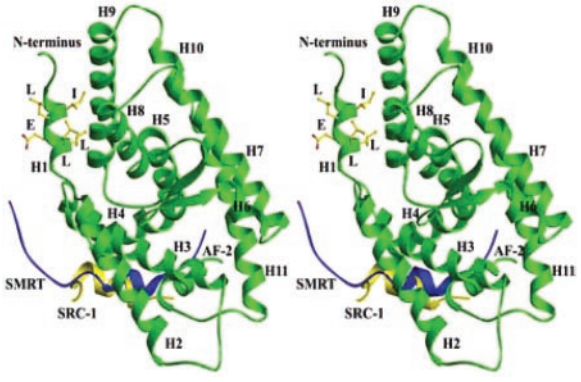

Fig. 3. A Stereoview of the Structural Model of hLRH-1 LBD.

The three-dimensional model of hLRH-1 LBD was built based on the crystal structure of mLRH-1 LBD (PDB entry 1PK5). The docked SRC-1 and SMRT peptides are shown in *yellow* and *purple*, respectively. Mutations of helix 1 are shown with side chains.

Coactivator SRC-1 Potentiates the Transcriptional Activity of hLRH-1

It is well documented that several transcriptional cofactors, including CBP, p300, SRC-1, and silencing mediator of retinoic acid and thyroid hormone receptors (SMRT), are often involved in the coregulation of NRs (17). We carried out cotransfection and reporter assays in Huh7 cells to examine whether any of these cofactors can affect the transcriptional activity of hLRH-1. The results show that SRC-1 can potentiate the activity of GAL4-hLRH-$1_{141–495}$ by about 2.7-fold; SMRT can repress it by about 3-fold, whereas CBP and p300 exhibit barely any effects (Fig. 4A). Similar results were obtained with reporter assays using pENII/CpLuc. SRC-1 can stimulate the reporter by 2.7-fold compared with hLRH-1 alone, whereas SMRT can repress it by 3.5-fold. CBP and p300 do not show any obvious effects (Fig. 4A).

The activation of the transcriptional activity of hLRH-1 by SRC-1 is significant because without the coexpression of SRC-1, even with an 8-fold GAL4-hLRH-$1_{141–495}$ expression plasmid, the reporter activity was still low (Fig. 4B). A Western blot was performed to rule out the possibility that the coexpression of SRC-1 might increase the expression of GAL4-hLRH-$1_{141–495}$, which could also enhance the reporter gene transcription. The results demonstrate that SRC-1 does not stimulate the expression of GAL4-hLRH-$1_{141–495}$, whereas the transfection with an 8-fold GAL4-hLRH-$1_{141–495}$ expression plasmid does induce an increased expression (Fig. 4C). Therefore, the coactivation of hLRH-1 by SRC-1 is due to a functional correlation between these two factors rather than through other secondary effects.

Multiple transcriptional factors can interact with the ENII/Cp region (43). To exclude the possibility that SRC-1 might activate the reporter pENII/CpLuc through other cellular factors instead of hLRH-1, a mutant reporter pENIIm/CpLuc was made, in which the critical hLRH-1 binding site in the ENII B1 element was mutated so that ENII is inert to the activation by hLRH-1 (15, 16). As expected, an overexpression of hLRH-1 could hardly activate this reporter. Coexpression of SRC-1 could not further stimulate the reporter

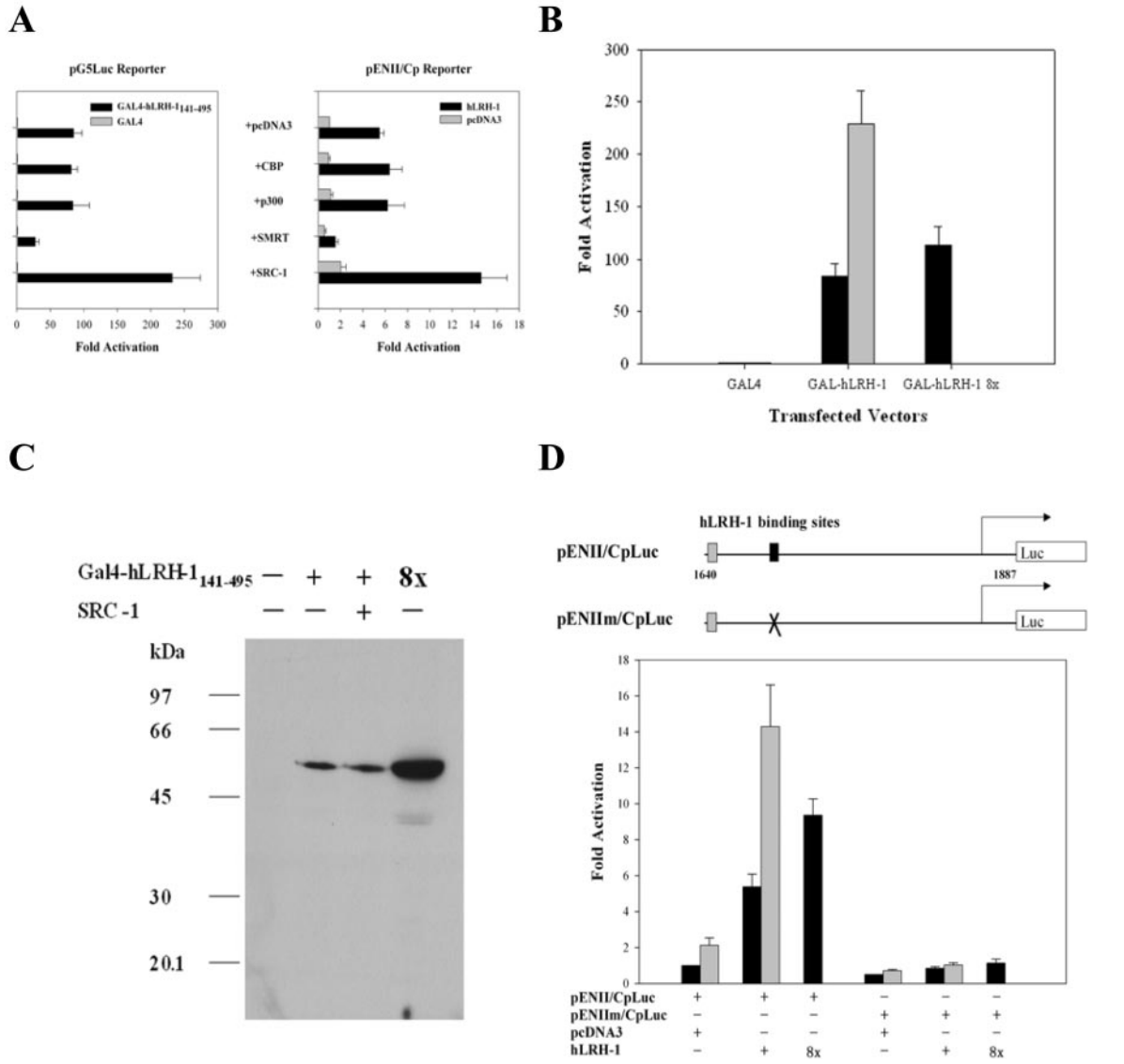

Fig. 4. Coactivator SRC-1 Potentiates the Transcriptional Activity of hLRH-1

A, Regulation of the hLRH-1 activity by one of the cofactors CBP, p300, SMRT, and SRC-1 was examined in Huh7 cells using (*left panel*) either the pG5Luc reporter (1 μg per dish) or (*right panel*) the pENII/CpLuc reporter (1 μg per dish). Expression plasmid of each cofactor (2 μg) was added to either pGAL4-hLRH-$1_{141–495}$ (0.2 μg) or pcDNA3-hLRH-1 (0.2 μg). Results are shown as fold activation above the basal activity (pGAL4-hLRH-$1_{141–495}$ or pcDNA3-hLRH-1, respectively), which is taken as 1. The average values with standard deviations from three independent duplicate experiments are shown. B, Potentiation of the hLRH-1 activity by the coexpression of SRC-1 (2 μg) and hLRH-1 (0.2 μg) is more significant than that resulted from the transfection with an 8-fold pGAL4-hLRH-$1_{141–495}$ (1.6 μg). The average values with standard deviations from three independent duplicate experiments are shown. C, Expression of GAL4-hLRH-$1_{141–495}$ fusion proteins was examined with Western blot assays. D, Specificity of the coactivation of hLRH-1 by SRC-1 was examined in Huh7 cells using either the wild-type or mutant ENII/Cp reporters (1 μg per dish). The SRC-1 expression plasmid (2 μg) was added to either 0.2 μg or 1.6 μg of pcDNA3-hLRH-1. Results are shown as fold activation above the basal activity (pcDNA3), which is taken as 1. The average values with standard deviations from three independent duplicate experiments are shown.

(Fig. 4D), suggesting that the coactivation by SRC-1 is primarily via hLRH-1. Cotransfection assay results performed in HeLa cells that lack endogenous hLRH-1 support the above suggestion. Despite a weak activation by hLRH-1 on the ENII/Cp in HeLa cells, coexpression of SRC-1 stimulates the reporter activity only in the presence of hLRH-1 (data not shown).

SRC-1 Physically Interacts with hLRH-1

The functional correlation between hLRH-1 and SRC-1 implicates that there might be a physical interaction between the two factors. To explore this possibility, a mammalian cell two-hybrid assay was firstly performed in Huh7 cells. A considerable activation of the reporter was

observed by the coexpression (Fig. 5A, *left panel*) of GAL4-hLRH-$1_{141–495}$ and VP16-SRC-1, in which the full-length SRC-1 was fused with the activation domain of VP16 (VP16-AD). A similar activation was observed in a reciprocal two-hybrid assay, in which the full-length SRC-1 was fused with the GAL4-DBD and the full-length hLRH-1 fused with the VP16-AD (Fig. 5A, *right panel*). Similar results were obtained from experiments in HeLa cells (data not shown). These data suggest an interaction between SRC-1 and hLRH-1 in mammalian cells.

The interaction can be a physical contact or mediated by a third party protein(s). To examine the property of the interaction, glutathione-*S*-transferase (GST) pull-down assays were performed. We were able to express the GST-hLRH-$1_{186–495}$ fusion protein in soluble form using the *Escherichia coli* system. Because aa 186–495 contain most of the hinge region and the complete LBD and shows an activity similar to that of aa 141–495 (Fig. 1B), we used the GST-hLRH-$1_{186–495}$ fusion protein in the pull-down assays. As shown in Fig. 5B, the immobilized GST-hLRH-$1_{186–495}$ could interact specifically with a ^{35}[S]-labeled *in vitro* translated full-length SRC-1. As a positive control, the GST-retinoic acid receptor (RAR) α fusion protein can interact strongly with the labeled SRC-1 only in the presence of its specific ligand all-*trans* retinoic acid

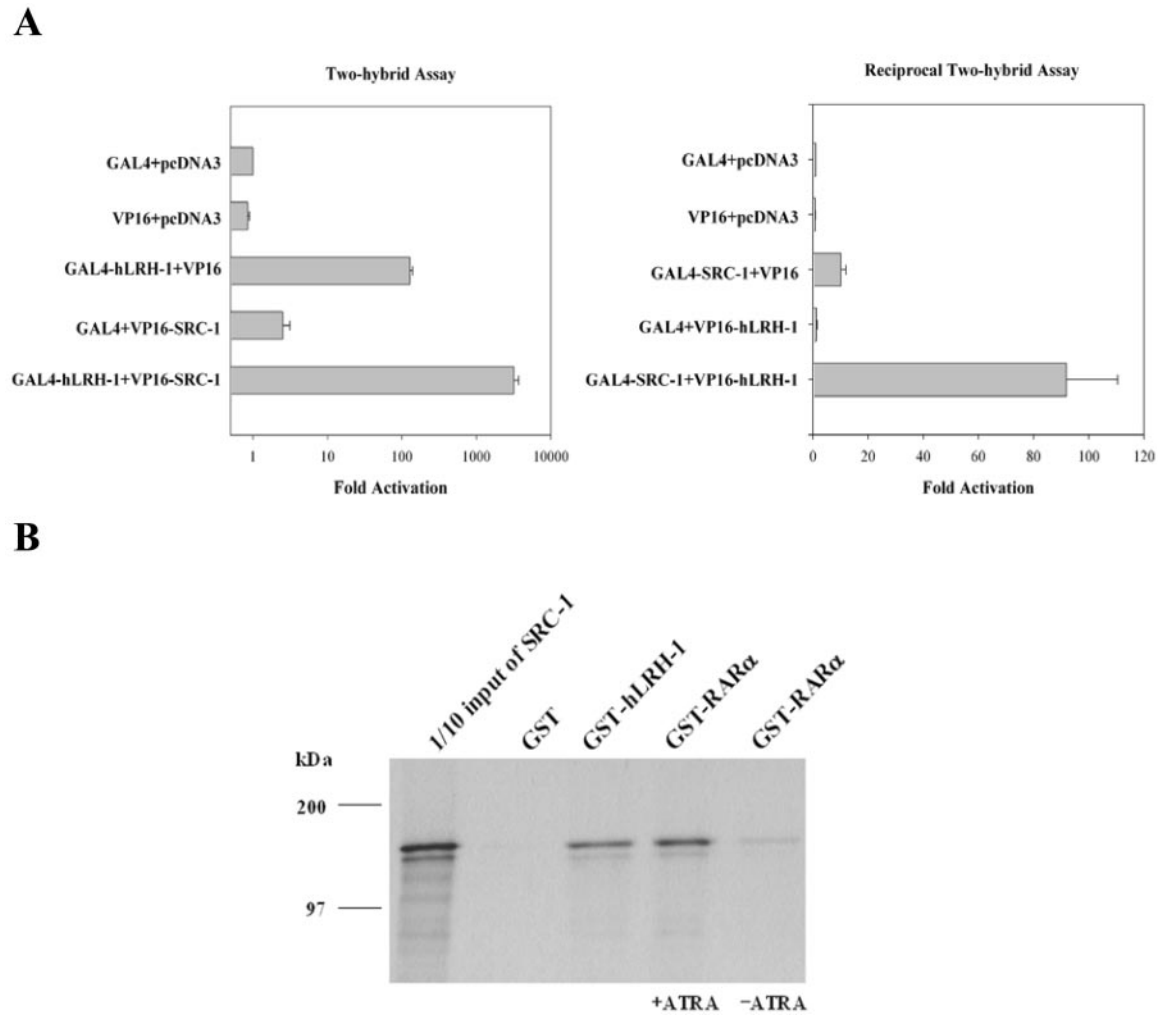

Fig. 5. SRC-1 Physically Interacts with hLRH-1

A, *Left panel,* Interaction between SRC-1 and hLRH-1 was tested by mammalian two-hybrid assays using the pG5Luc reporter (0.5 μg per dish). Huh7 cells were transfected with 1 μg empty vectors (pM and pVP16), or pM and pVP16-SRC-1, or pVP16 and pGAL4-hLRH-$1_{141–495}$, or pVP16-SRC-1 and pGAL4-hLRH-$1_{141–495}$. *Right panel*, Interaction between SRC-1 and hLRH-1 was also tested by reciprocal mammalian two-hybrid assays using the pG5Luc reporter (0.5 μg per dish). Results are shown as fold activation above the basal activity (pM and pVP16), which is taken as 1. The average values with SD from three independent duplicate experiments are shown. B, Direct interaction between SRC-1 and hLRH-1 was tested by GST pull-down assays. Either GST or GST-hLRH-$1_{186–495}$ protein was incubated with the ^{35}[S]-labeled *in vitro* translated full-length SRC-1. GST-RARα was incubated with the labeled full-length SRC-1 in the presence or absence of the ligand ATRA (2 μM). The lane on the *left* contains one tenth the amount of the SRC-1 protein used in all incubations.

(ATRA). No interaction was observed between GST alone and SRC-1. These results clearly suggest that SRC-1 interacts directly with hLRH-1 and that the interaction might occur in the absence of a ligand or any posttranslational modifications of hLRH-1.

The Region Containing the Q-Rich Domain of SRC-1 Is Primarily Involved in Its Interaction with hLRH-1

To characterize the region of SRC-1 involved in its interaction with hLRH-1, several truncated SRC-1 were fused to GST. The truncated SRC-1 were designed to contain specific regions that have been reported to be important in protein-protein interaction and transcriptional regulation, including the basic-helix-loop-helix/Per/ARNT/Sim (bHLH-PAS) domain, nuclear receptor-interacting domain (NID), CBP/P300-interacting domain (AD1), Q-rich domain, and activation domain 2 (AD2) (44) (Fig. 6A). Pull-down assays were performed with the ^{35}[S]-labeled *in vitro* translated full-length hLRH-1. As shown in Fig. 6B, strong interactions exist between hLRH-1 and GST-SRC-$1_{1029–1255}$ or GST-SRC-$1_{1255–1441}$. The interactions between hLRH-1 and GST-SRC-$1_{568–780}$ or GST-SRC-$1_{1321–1441}$ are much weaker. Other GST-SRC-1 fusion proteins, as well as GST alone, do not display any interactions with hLRH-1.

Mammalian two-hybrid assays were then performed to verify the pull-down assay results. Full-length and fragments of SRC-1 were fused with the VP16-AD. Each fusion protein was coexpressed with GAL4-hLRH-$1_{141–495}$ in Huh7 cells (Fig. 6C). Marked activations of the reporters were observed with the full-length, aa 1029–1255, and aa 1255–1441 of SRC-1, whereas slight activations were detected with aa 568–780 and aa 1321–1441. No activation was observed with other truncated SRC-1 proteins. These results are consistent with the data from the pull-down experiments.

The NID of SRC-1 is implicated in mediating the interaction between SRC-1 and nuclear receptors through its internal LXXLL motifs (45). However, our data show that there is only a weak interaction between the NID of SRC-1 (aa 568–780) and hLRH-1. To further assess the role of the NID in the interaction, a full-length SRC-1 containing a mutant NID (NIDm) was made, in which all three LXXLL motifs in the NID were replaced by LXXAA (Fig. 6D). As shown in Fig. 6E, the interaction between the NIDm and hLRH-1 remains strong. In contrast, the interaction between the NIDm and RARα is significantly impaired, consistent with the biochemical data that the NID is required for the interaction with RARα (35). These results demonstrate that the NID of SRC-1 plays a minor role for its interaction with hLRH-1.

Cotransfections with the expression plasmids of GAL4-hLRH-$1_{141–495}$ and mutant SRC-1 support the pull-down assay results. As shown in Fig. 6F, SRC-1 containing the mutant NID can still coactivate hLRH-1, though to a somewhat lesser extent compared with the wild-type SRC-1. Both SRC-$1_{1–1321}$ and SRC-$1_{1–1255}$ exhibit similar coactivation capabilities as the wild-type SRC-1, whereas SRC-$1_{1–1029}$ and SRC-$1_{d1029–1255}$ do not stimulate hLRH-1. Similar results were obtained from the cotransfection assays with the pENII/CpLuc reporter. Moreover, GST pull-down assay using SRC-$1_{d1029–1255}$ indicates that the aa 1029–1255 deletion abrogates the binding of SRC-1 to GST-hLRH-$1_{186–495}$, whereas it does not affect the binding of SRC-1 to GST-RARα (Fig. 6E). Collectively, SRC-1 interacts directly with hLRH-1 primarily via the C-terminal region aa 1029–1255 that contains the Q-rich domain.

Both Helix 1 and AF-2 of hLRH-1 Are Important for the Recruitment of SRC-1

Both AF-2 and helix 1 of hLRH-1 are essential for its transcriptional activity. Whether these structural elements are also required for the recruitment of SRC-1 was investigated by mammalian two-hybrid assays. Several GAL4-hLRH-1 fusion proteins (as in Fig. 1B) were examined for their potential interactions with VP16-SRC-1. Obvious interactions were observed with aa 141–495, aa 219–495, and aa 256–495 of hLRH-1. In contrast, no interaction was observed with those truncated hLRH-1s in which either helix 1 (aa 262–495) or AF-2 (aa 141–481) was disrupted or partially deleted (Fig. 7A).

Next, pull-down assays were performed with the immobilized GST-SRC-$1_{1029–1255}$ and the labeled *in vitro* translated full-length hLRH-1 containing point mutations in helix 1 or AF-2 (depicted in Fig. 2B). Compared with wild-type hLRH-1, the $E_{261}G$ mutant displays a weaker interaction with GST-SRC-$1_{1029–1255}$, whereas other mutants, namely $IL_{260}AA$, $LL_{263}AA$, and AF-2del, show much more severe impairment in the interaction (Fig. 7B). The data are well consistent with the reporter assay results shown in Fig. 2C, indicating that the more severe the activity is affected by the mutations, the weaker the interaction is between hLRH-1 and SRC-1. Moreover, based on the weak interactions between SRC-1 and the hLRH-1 mutants containing point mutations in helix 1, it can be deduced that the interaction between AF-2 and SRC-1 is weak. Collectively, these data indicate that both helix 1 and AF-2 of hLRH-1 play important roles in the recruitment of SRC-1.

Interestingly, overexpression of SRC-1 could dramatically enhance the transcriptional activities of those hLRH-1 mutants that contain point mutations of the hydrophobic residues in helix 1 (Fig. 7C). The GAL4-hLRH-$1_{141–495}$ containing $IL_{260}AA$ or $LL_{263}AA$ mutations have very weak transcriptional activities in Huh7 cells. However, if SRC-1 was coexpressed, the activities of these mutants could increase dramatically by about 12- and 16-fold, respectively. Although the coexpression of SRC-1 did not rescue the transcriptional activity of the AF-2 partial deletion mutant, it seems that the overexpression of SRC-1 can partially compensate the impaired interactions between SRC-1

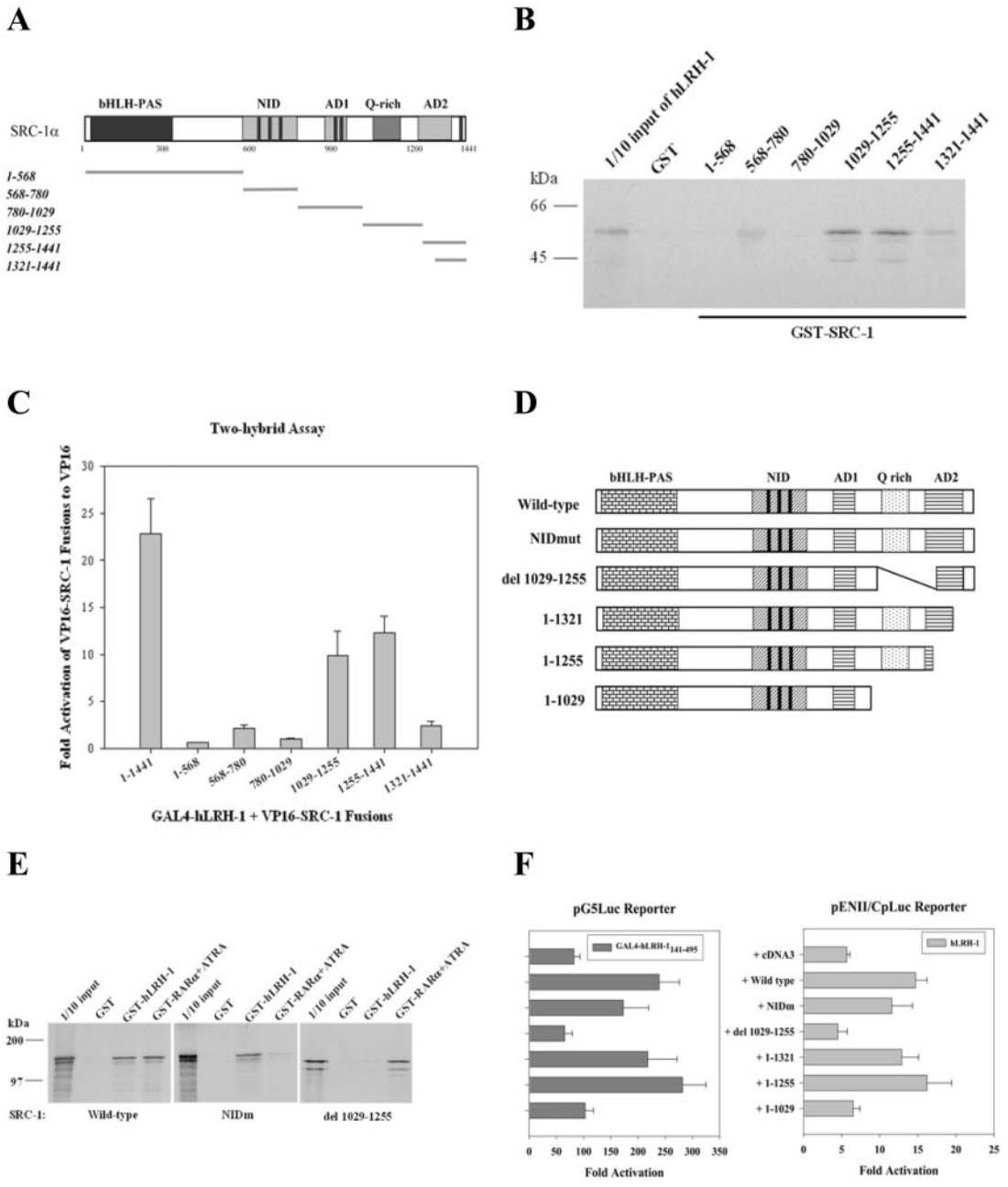

Fig. 6. The Region Containing the Q-Rich Domain of SRC-1 Is Primarily Involved in Its Interaction with hLRH-1

A, Schematic representation of the domains in SRC-1. The bHLH-PAS, NID, AD1, AD2, and Q-rich are depicted. The *lines below* represented the SRC-1 fragments used in GST pull-down assays. B, Interaction between each SRC-1 fragment and hLRH-1 was tested by GST pull-down assays. GST or each GST-SRC-1 fusion protein was incubated with the (35)[S]-labeled *in vitro* translated full-length hLRH-1. The lane on the *left* contains one tenth the amount of the hLRH-1 protein used in all incubations. C, Interaction between each SRC-1 fragment and hLRH-1 (1 μg each) was also examined by mammalian two-hybrid assays using the pG5Luc reporter (0.5 μg per dish). Results are shown as fold activation above the basal activity (pGAL4-hLRH-$1_{141–495}$ and pVP16), which is taken as 1. The average values with standard deviations from three independent duplicate experiments are shown. D, Schematic representation of the SRC-1 mutants that contain point mutations in the NID (NIDm), an internal deletion of aa 1029–1255, and C-terminal truncations (aa 1–1029, aa 1–1255, and aa 1–1321). E, Interaction between each SRC-1 mutant and hLRH-1 was tested by GST pull-down assays. GST or GST-hLRH-$1_{186–495}$ was incubated with each ^{35}[S]-labeled *in vitro* translated SRC-1 mutant. GST-RARα was incubated with each labeled SRC-1 mutant in the presence of ATRA (2 μM). The lane on the *left* contains one tenth the amount of each SRC-1 protein used in all incubations. F, Regulation of the hLRH-1 activity by SRC-1 mutants was tested in Huh7 cells using the pG5Luc reporter (1 μg per dish, *left panel*) and the pENII/CpLuc reporter (1 μg per dish, *right panel*). The expression plasmid of each SRC-1 mutant (2 μg) was added to 0.2 μg of pGAL4-hLRH-$1_{141–495}$ (*left panel*) or pcDNA3-hLRH-1 (*right panel*). Results are shown as fold activation above the basal activity (pGAL4-hLRH-$1_{141–495}$ and pCR3.1), which is taken as 1. The average values with SD from three independent duplicate experiments are shown.

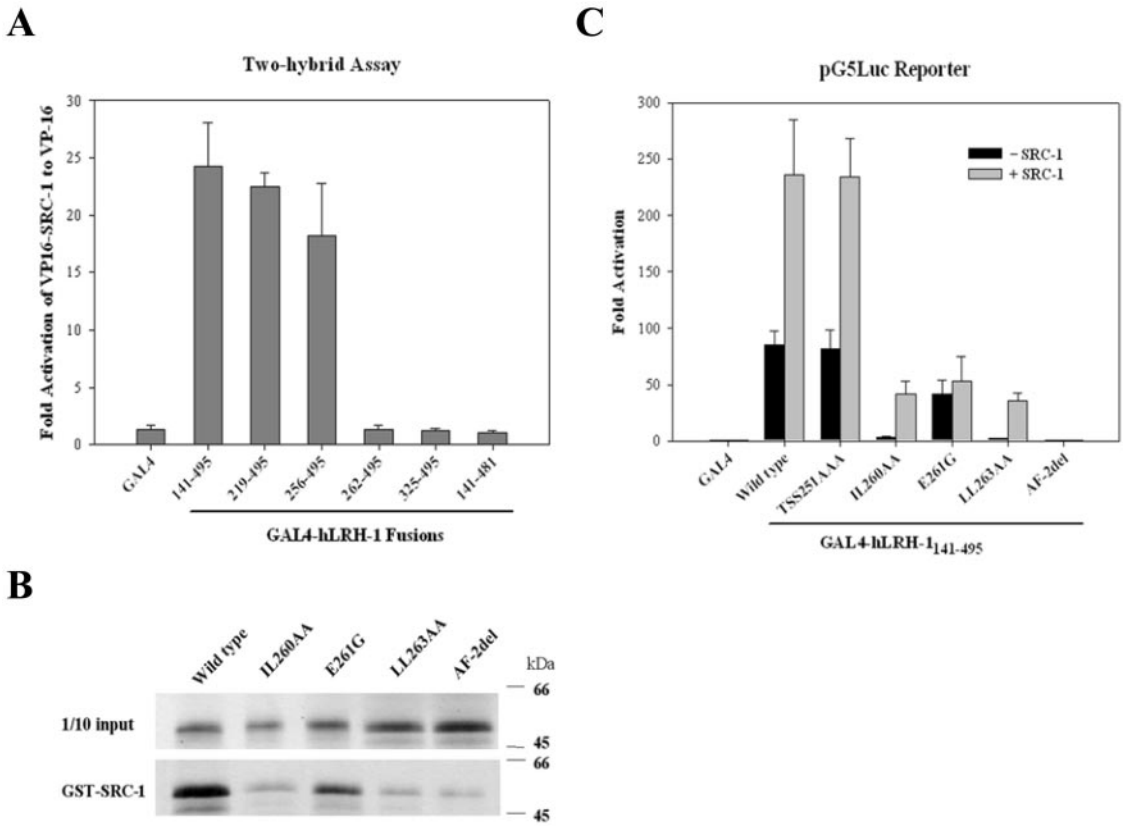

Fig. 7. Both helix 1 and AF-2 of hLRH-1 Are Important for the Recruitment of SRC-1.

A, Interaction between each truncated hLRH-1 and SRC-1 (1 μg each) was tested by mammalian two-hybrid assays using the pG5Luc reporter (0.5 μg per dish). Results are shown as fold activation above the respective basal activity (each GAL4-hLRH-1 fusion protein and pVP16), which is taken as 1. The average values with standard deviations from three independent duplicate experiments are shown. B, Interaction between each truncated hLRH-1 and SRC-1 was also examined by GST pull-down assays. GST or GST-SRC-$1_{1029–1255}$ was incubated with each ^{35}[S]-labeled *in vitro*-translated hLRH-1 protein. The *upper panel* represented one tenth the amount of each hLRH-1 protein used in the respective incubation. C, SRC-1 could partially rescue the activities of the hLRH-1 mutants in cotransfection assays using the pG5Luc reporter (1 μg per dish). The SRC-1 expression plasmid (2 μg) was added to each expression plasmid of either wild-type or mutant GAL4-hLRH-$1_{141–495}$ (0.2 μg). Results are shown as fold activation above the basal activity (pM and pcDNA3), which is taken as 1. The average values with SD from three independent duplicate experiments are shown.

and hLRH-1 mutants that contain point mutations of the hydrophobic residues in helix 1.

SRC-1 Potentiates hLRH-1-Mediated Activation of the CYP7A1 Promoter

To further demonstrate the physiological relevance of SRC-1 for hLRH-1 signaling, we investigate whether SRC-1 can potentiate hLRH-1 mediated activation of the liver-specific CYP7A1 promoter and the transcription of the endogenous CYP7A1 gene in hepatic cells. A consensus hLRH-1 binding site is located in the core promoter of hCYP7A1 gene (11). A reporter assay was first performed as previously done with the ENII/Cp promoter. As shown in Fig. 8A, hLRH-1 and SRC-1 activated a CYP7A1 promoter reporter about 2.9- and 1.6-fold, respectively. However, when coexpressed with hLRH-1, SRC-1 enhanced the reporter activity up to 8-fold, indicating that SRC-1 can potentiate hLRH-1-dependent activation of the CYP7A1 promoter. To investigate whether overexpression of SRC-1 has an impact on the transcription of the endogenous CYP7A1 gene, semiquantitative RT-PCR assays were performed. As shown in Fig. 8B, overexpression of hLRH-1 or SRC-1 increased the transcription of the endogenous CYP7A1 slightly in Huh7 cells. When coexpressed with hLRH-1, SRC-1 could increase the transcription of the endogenous CYP7A1 up to 60%. Taken together, SRC-1 can potentiate hLRH-1-mediated activation of the transcription of the CYP7A1 gene.

TIF2 and ACTR Also Interact Physically with hLRH-1 and Potentiate Its Transcriptional Activity

All members of the SRC family share a moderate sequence similarity (50–55%) and a higher similarity in

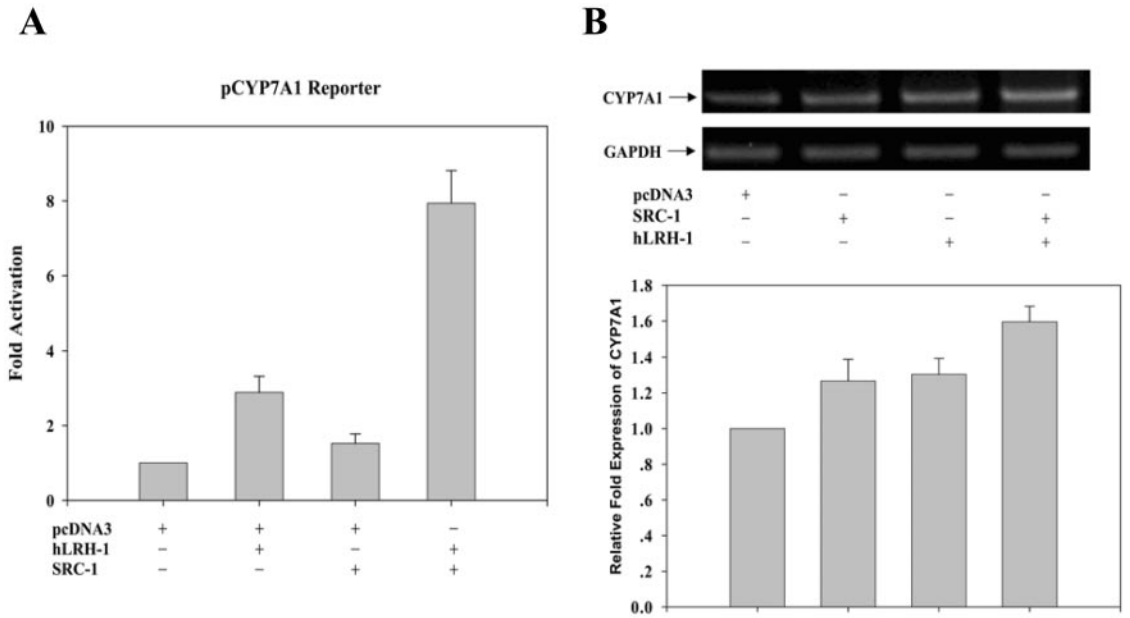

Fig. 8. SRC-1 Potentiates hLRH-1-Mediated Activation of the CYP7A1 Promoter

A, Potentiation of the hLRH-1 activity on hCYP7A1 promoter by SRC-1 was investigated in Huh7 cells by the coexpression of SRC-1 (2 μg) and pcDNA3-hLRH-1 (0.2 μg). Transfection with either the SRC-1 (2 μg) or the hLRH-1 (0.2 μg) expression plasmid was performed in comparison. Results are shown as fold activation above the basal activity (pcDNA3), which is taken as 1. The average values with standard deviations from three independent duplicate experiments are shown. B, Semiquantitative RT-PCR was used to determine the relative levels of the CYP7A1 transcript among different transfection assays. Huh7 cells were transfected with either the SRC-1 (6 μg) or the hLRH-1 (3 μg) expression plasmid or both using the FuGene 6 reagent. The control cells were transfected with pcDNA3. A representative PCR is shown (*upper panel*). The expression of CYP7A1 is normalized with that of GAPDH. Results are shown as relative fold expression of CYP7A1 with that from control cells taken as 1. Data from at least three RT-PCR assays were calculated and presented ($P < 0.01$) (*lower panel*).

structure features, and may have functional redundancies in tissues where they coexpress (46). SRC-1, TIF2, and ACTR mRNAs have been detected in many tissues, including liver and pancreas where predominant hLRH-1 expression exists (28, 32–34, 47–50) and all three SRC proteins have been detected in liver by Western blot (29, 49). RT-PCR analysis showed that Huh7 cells have inherent expression of all three SRCs as well as hLRH-1 (Fig. 9A). It is thus interesting to investigate whether TIF2 and ACTR can also interact with hLRH-1 and potentiate its transcriptional activity in a similar manner as SRC-1. Cotransfection analysis was performed in Huh7 cells. The activity of GAL4-hLRH-$1_{141–495}$ was enhanced by all three SRCs with TIF2 showing a dramatic potentiation (up to 13.5-fold) (Fig. 9B). Similar results were obtained using the ENII/Cp reporter (data not shown). Potentiation of hLRH-1 activity by all three SRCs was also observed in cotransfection assays with the CYP7A1 promoter reporter (Fig. 9C). However, with the CYP7A1 promoter, TIF2 did not show a dramatic potentiation, which was different from the results performed with the GAL4 based reporter and the pENII/CpLuc reporter. Thus, the relative strength of potentiation by different SRCs appears to depend on the promoter used.

Because AD1 of SRC-1 can recruit CBP/p300 (51), we asked whether CBP might enhance the coactivation of hLRH-1 mediated by SRCs. CBP alone did not potentiate the activity of GAL4-hLRH-$1_{141–495}$. However, when coexpressed with SRC-1 or ACTR, CBP could enhance the transcriptional activity of GAL4-hLRH-$1_{141–495}$ (Fig. 9B), suggesting that CBP might be recruited by SRC-1 or ACTR. Interestingly, CBP failed to enhance TIF2 mediated coactivation of hLRH-1.

To investigate a possible physical interaction between hLRH-1 and TIF2 or ACTR, GST pull-down assays were performed using GST-hLRH-$1_{186–495}$ and *in vitro*-translated TIF2 or ACTR. Similar to SRC-1, both TIF2 and ACTR interact with hLRH-1 directly (Fig. 9D). Subsequently, the interaction regions between hLRH-1 and TIF2 or ACTR were investigated with mammalian two-hybrid and GST pull-down assays. Because C-terminal domains (AD1, Q-rich, and AD2) are less conserved in sequence among SRCs (46), we tethered the part beginning from the Q-rich region to the C-terminal of TIF2 or ACTR with GAL4-DBD. As shown in Fig. 9E, the C-terminal part of TIF2 or ACTR interacts with hLRH-1 in Huh7 cells. The interaction is abrogated when helix 1 or AF-2 of hLRH-1 LBD was deleted. GST pull-down assays also revealed that NID of TIF2 or ACTR interacts with hLRH-1 weakly, although it interacts with ligand-bound RARα strongly (Fig. 9F). Therefore, the interaction between hLRH-1 and TIF2 or ACTR is similar to that between hLRH-1

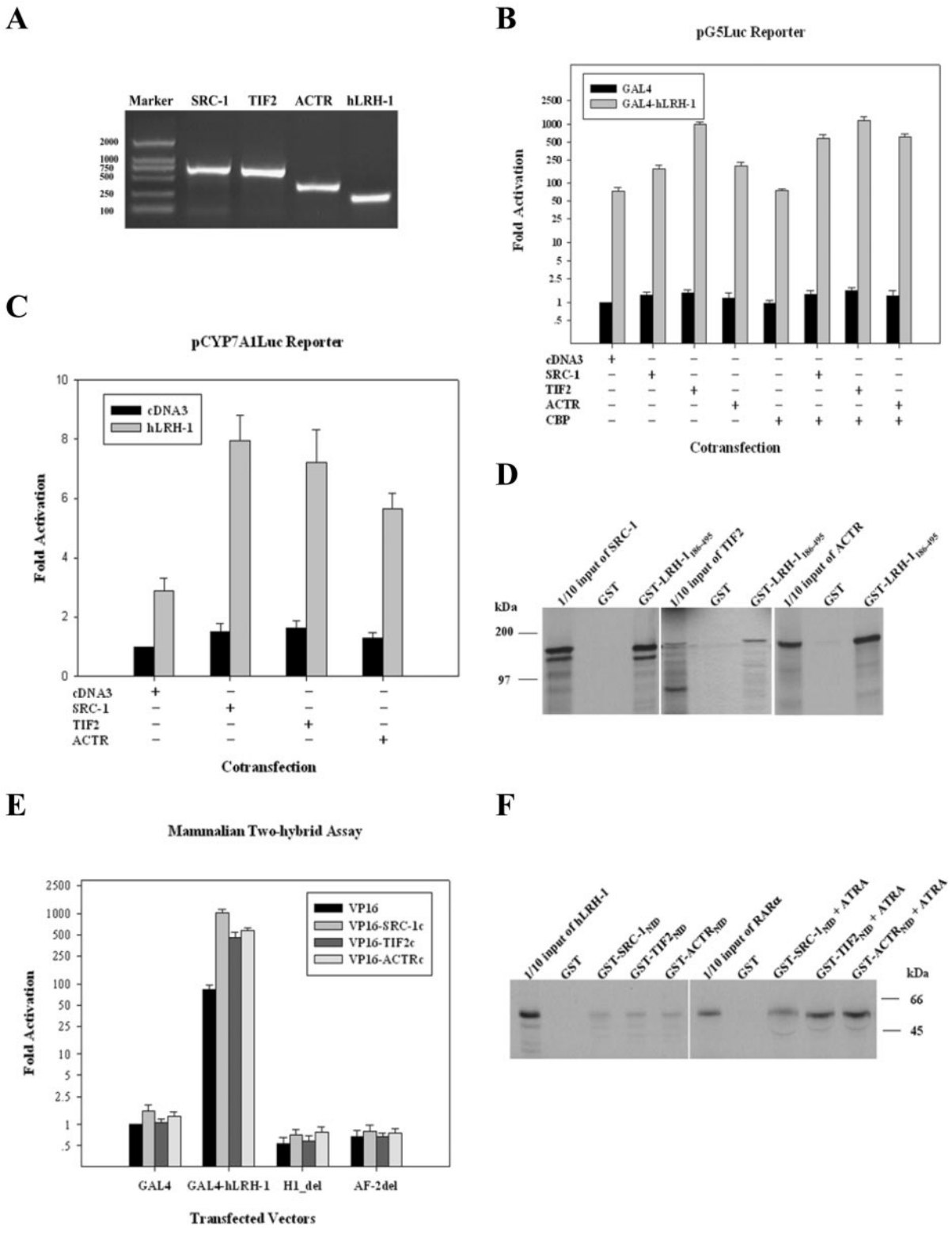

Fig. 9. TIF2 and ACTR Also Interact Physically with hLRH-1 and Potentiate Its Transcriptional Activity

A, The endogenous expression of SRC-1, TIF2, ACTR, and hLRH-1 in Huh7 cells were examined by RT-PCR. Fragments corresponding to the C-terminal region of SRCs were amplified (SRC-1, 681 bp; TIF2, 603 bp; ACTR, 327 bp). For hLRH-1, the amplicon is within the hinge region (219 bp). B, Potentiation of the hLRH-1 activity by SRCs was examined in Huh7 cells using the pG5Luc reporter (1 μg per dish). Expression plasmid of each SRC (2 μg) was added to pGAL4-hLRH-$1_{141–495}$ (0.2 μg). To examine whether the coactivation of the hLRH-1 activity by SRCs is enhanced by CBP, the CBP expression plasmid (1 μg) was added to pGAL4-hLRH-$1_{141–495}$ (0.2 μg) in the presence or absence of each SRC (2 μg). Results are shown as Log (10) value of

and SRC-1. Take together, these results suggest a functional redundancy among members of SRC family in the potentiation of the transcriptional activity of hLRH-1.

DISCUSSION

Similar to other NRs, hLRH-1 is composed of several modular functional domains. We demonstrate here that in addition to AF-2, helix 1 (aa 257–264) of the LBD is also essential for the transcriptional activity of hLRH-1. A recent study has also revealed a crucial function of a homologous helix 1 for the transcriptional activity of SF-1, which is consistent with our data (52). The function of helix 1 thus seems conserved among FTZ-F1 related receptors. In addition, we have also discovered other potential regulatory domains in the hinge region of hLRH-1, including a strong repression element (aa 219–227) that has also been found in SF-1 (22). Sequence analyses reveal that this element is unique to the FTZ-F1 related receptors. It has been reported that DP103, a DEAD box protein, interacts with the equivalent region of SF-1, though the exact mechanism of the repression is not clear (22). Because DP103 is expressed in relatively low amount in liver as detected by Northern blot (22), it remains to be assessed whether DP103 or a related protein interacts with the repression element of hLRH-1 and exerts the repression effect.

Many coregulators have been documented to potentiate or repress the activities of NRs through direct or indirect interactions (17). Several factors including Dax-1, CBP/p300, TReP-132, DP103 (19–22), and SRC-1 (39, 40) have been implicated in modulating the transcriptional activity of SF-1. Small heterodimer partner has been found to interact with AF-2 of mLRH-1 and represses its transcriptional activity in bile acid synthesis (53). Here we demonstrate that SRC-1 as well as its homologous coactivators TIF2 and ACTR interact directly with hLRH-1 and potentiate the transcriptional activity of hLRH-1 on GAL4 responsive reporter, HBV ENII/Cp, and the CYP7A1 promoter. Moreover, overexpressed SRC-1 enhances the endogenous transcription of the CYP7A1 gene in Huh7 cells, although not as significantly as it does on the CYP7A1 promoter reporter, which probably due to a much tighter regulation of the endogenous CYP7A1 expression in cells. Because the purified *E. coli*-expressed hLRH-1 is capable of interacting with the *in vitro* translated SRCs, it seems that the interaction can occur in the absence of a potential ligand. SRC-1 has also been shown to coactivate SF-1. Nevertheless, a direct interaction between SF-1 and SRC-1 has not been clearly demonstrated yet (39, 40). For SF-1, the phosphorylation of residue S203 in the hinge region by the MAPK pathway maximizes the SF-1 mediated transcription and its interaction with cofactors (23). Because the hinge region is the least conserved region ($<$25% sequence identity) between SF-1 and hLRH-1, whether a similar phosphorylation mechanism exists for hLRH-1 awaits future investigation.

SRC-1 contains several functional domains, including a basic bHLH-PAS domain, a central nuclear receptor interacting domain (NID), a loosely defined Q-rich domain, and two activation domains (44). The NID features three LXXLL motifs (NR box) that have been demonstrated to be necessary and sufficient for mediating the direct interaction between SRC-1 and several ligand-bound NRs, such as RARα and estrogen receptor (ER) (35, 45). This appears not the case for hLRH-1. Our data show that strong physical and functional interactions are mainly observed between hLRH-1 and the aa 1029–1255 region of SRC-1 that contains the Q-rich domain. Deletion of this region results in complete loss of the interaction and thus the coactivation of hLRH-1. In contrast, the NID of SRC-1 (aa 568–780) is shown to have only a weak interaction with hLRH-1 in cells and *in vitro*. Mutations of the LXXLL motifs in the NID do not obviously alter the interaction between SRC-1 and hLRH-1 and have only a minor effect on SRC-1 coactivation. Therefore, the NID of SRC-1 plays a minor role in its interaction and coactivation of hLRH-1. The Q-rich domain of SRC-1

fold activation above the basal activity (pGAL4-hLRH-$1_{141–495}$), which is taken as 1. The average values with standard deviations from three independent duplicate experiments are shown. C, Potentiation of the hLRH-1 activity by SRCs was also examined in Huh7 cells using the CYP7A1 promoter reporter (1 μg per dish). Expression plasmid of each SRC (2 μg) was added to pcDNA3-hLRH-1 (0.2 μg). Results are shown as fold activation above the basal activity (pcDNA3-hLRH-1), which is taken as 1. The average values with SD from three independent duplicate experiments are shown. D, Direct interaction between hLRH-1 and TIF2 or ACTR was tested by GST pull-down assays. Either GST or GST-hLRH-$1_{186–495}$ protein was incubated with the ^{35}[S]-labeled *in vitro* translated full-length TIF2 or ACTR. GST-hLRH-$1_{186–495}$ protein incubated with the labeled full-length SRC-1 was also performed alongside. The input lanes contain one tenth the amount of SRC-1, TIF2, and ACTR used in pull-down assays, respectively. E, Regions responsible for the interaction between hLRH-1 and TIF2 or ACTR were investigated by mammalian two-hybrid assays using the pG5Luc reporter (0.5 μg per dish). Huh7 cells were transfected with indicated expression plasmids or empty vectors (1 μg each). Results are shown as fold activation above the basal activity (pM and pVP16), which is taken as 1. The average values with standard deviations from three independent duplicate experiments are shown. F, Interaction between hLRH-1 and the NID of TIF2 or ACTR was tested by GST pull-down assays. GST or the NID of each SRC fused with GST was incubated with the ^{35}[S]-labeled *in vitro*-translated hLRH-1 or RARα in the presence of the ligand ATRA (2 μM). Equal amount of each GST-NID protein was applied as estimated by SDS-PAGE (data not shown). The input lanes contain one tenth the amount of hLRH-1 or RARα used in pull-down assays.

can mediate the ligand-independent activity of the androgen receptor (54, 55). However, in that case, it is the N-terminal AF-1 domain of the androgen receptor that is involved in interaction and potentiation. Therefore, this is the first report that SRC-1 can interact with the LBD of an NR by means of a region containing the Q-rich domain. On the other hand, aa 1–1255 of SRC-1 that does not contain AD2 is fully active in potentiating hLRH-1, suggesting that AD2 is not necessary for the coactivation of hLRH-1. However, it is noteworthy that AD2 (as in aa 1255–1441) of SRC-1 can interact with hLRH-1 under our experimental conditions. The same region was previously shown to have interactions with SF-1 in a mammalian two-hybrid assay (39, 40). Therefore, we cannot exclude the possibility that AD2 is also required in specific cell types or for other hLRH-1-dependent promoters because it has been reported that the function of AD2 may depend on the context of cell types and promoters (38, 44).

Structural and biochemical studies of mLRH-1 LBD suggest that the cofactor recruitment by the conserved core structure is not optimized and the binding of coregulators to mLRH-1 is relatively weaker than to other NRs (41). To enhance cofactor recruitment, other structural modules may be required to provide additional stabilizing forces. Indeed, our data show that in addition to AF-2 that is usually involved in coactivator recruitment, helix 1 of hLRH-1 LBD is also essential for the transcriptional activity of hLRH-1 and plays an important role in the recruitment of SRC-1. Point mutations in helix 1 would impair its interaction with SRC-1 and reduce the transcriptional activity of hLRH-1, suggesting that AF-2 of hLRH-1 has a relatively weak interaction with SRC-1. Structural comparisons of several NRs [RAR-related orphan receptor, retinoid X receptor (RXR), peroxisome proliferator-activated receptor (PPAR), ER, and RAR] and the structural model of hLRH-1 indicate that the sandwich framework of NR structures is well conserved. Helix 1 is located at the N terminus of the LBD, is exposed on the outer surface, and forms part of the sandwich framework. The only structural element that has a great flexibility is the region that comprises helix 2. Docking experiments based on the crystal structure of several NR LBDs in complexes with SRC-1 or SMRT peptides containing the conserved LXXLL motif indicate that both SRC-1 and SMRT peptides can bind to hLRH-1 LBD in the surface cleft formed by helices 3 and 4 and AF-2 (Figs. 3 and 10). However, as in mLRH-1, the residues that compose the coactivator-binding cleft in hLRH-1 comprise four residues (R315, M329, Q398, and N484) different from those in other receptors. R315 forms part of the so-called "electrostatic clamp" that stabilizes the receptor-coactivator complex (56). The corresponding residue in other receptors is lysine. In the structural model of hLRH-1 LBD with docked SRC-1 peptide, the side chain of R315 has steric conflict

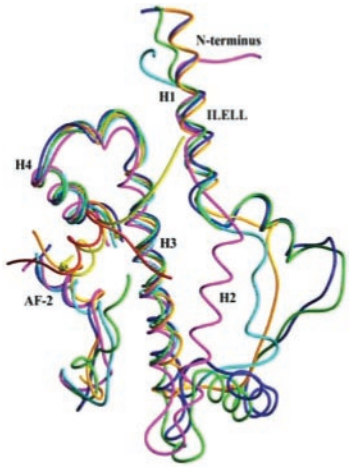

Fig. 10. Superposition of the LBDs of Several NRs

The structure model of hLRH-1 LBD is shown in *magenta*. The crystal structures of PPARγ (PDB entry 1K74), RAR (PDB entry 1K4W), and RXR (PDB entry 1K74) in complexes with the SRC-1 peptide are shown in *green*, *blue*, and *cyan*, respectively; the structure of PPARγ (PDB entry 1KKQ) in complex with the SMRT peptide is shown in *gold*. The bound SRC-1 fragment is shown in *red* and the SMRT fragment in *yellow*.

with one of the conserved leucine residues of the SRC-1 peptide. M329 and N484 have relatively large side chains compared with the usually smaller residues (A/S/T/V/P) at these positions in other receptors and appear to also have close contacts with the docked SRC-1 peptide. Mutations of these two residues in mLRH-1 to the smaller residues in RXR (M394V/N549T) increase significantly the activation of mutant mLRH-1 by other NR coregulators (41). Therefore, the amino acid differences at these positions appear to be primarily responsible for the weak interactions between SRC-1 and AF-2 of mouse and hLRH-1. On the other hand, the modeling studies show that the C terminus of SMRT fragment runs across helix 3 and extends further to reach helix 1 and has the potential to interact with the ILELL segment of helix 1. It is conceivable that SRC-1 may also extend along the same path and has interactions with helix 1 of LBD during coactivation.

Based on the structural and mutagenesis studies, we propose here a model that LRH-1 might employ to recruit SRC-1. In other NRs, SRC-1 runs across AF-2, helices 3 and 4, and possibly helix 1, but mainly interacts with AF-2 due to the optimized coactivator-binding cleft. In human and mouse LRH-1, however, the interaction between AF-2 and SRC-1 is relatively weaker owing to the unoptimized binding cleft. Thus, helix 1 may act to pull SRC-1 closer and forms stronger direct interactions. In this regard, the $IL_{260}AA$ or $LL_{263}AA$ mutations can slightly alter the precise position of helix 1 and reduce partially its interactions with SRC-1. Coex-

pression of SRC-1 with hLRH-1 mutants containing point mutations in helix 1 likely stabilizes the conformation and position of helix 1 and compensate the weakened interactions resulted from these mutations. X-ray crystallographic analysis of the hLRH-1 LBD in complex with SRC-1 should provide detailed structural information.

Three homologous members of the SRC family have been identified in human and rodents, which produce proteins about 160 kDa in size and have an overall sequence similarity of 50–55% among them. They share high homology in functional domain, including bHLH-PAS, NID, AD1, AD2, and Q-rich domain. All three SRCs have been detected by Northern blot in many tissues including liver and pancreas where hLRH-1 expression is enriched. Protein-protein interaction assays have indicated that SRCs share many common features that permit interaction with and coactivation of NRs (45, 56, 57). Nevertheless, functional specificity among SRCs is still apparent based on the studies with SRC knockout (KO) mice. For example, partial resistance to steroid and thyroid hormones was observed in SRC-1 KO mice, whereas development of reproductive functions seems impaired in TIF2 and ACTR KO mice (49, 58, 59). It is likely that selective recruitment of SRCs by different NRs may mediate specific transcription signals. On the other hand, the viable phenotypes of SRC KO mice suggest that SRC family members may be able to partially compensate each other's function *in vivo* (49, 50, 60). The expression of known LRH-1 target genes has so far not been examined in SRC KO mice. In this study, all three SRCs share similar unique features in the interaction with hLRH-1, suggesting a functional redundancy among SRC family members in the potentiation of the transcriptional activity of hLRH-1. As a relatively new receptor, the number of known target genes of LRH-1 is still limited. Thus, it is also possible that some of the reported phenotypes with SRC KO mice may be directly or indirectly related to LRH-1 signaling. Identification of more LRH-1 target genes and careful examination on the expression of LRH-1 target genes in SRC KO mice may provide important information on the *in vivo* functional interaction between LRH-1 and SRCs.

Interestingly, in our cotransfection analyses, TIF2 shows a relatively greater potential in coactivating hLRH-1 than SRC-1 and ACTR on the pG5Luc and pENII/CpLuc reporters, but not on the CYP7A1 promoter reporter. Coexpression of CBP and SRC-1 or ACTR shows an elevated hLRH-1 activity , whereas this is not the case in the coexpression of CBP and TIF2, which is also observed in COS cells (data not shown). Because no obvious difference exists in the interaction with hLRH-1 among three SRCs in our studies, the different coactivation of hLRH-1 by SRCs on different promoters may be caused by selective recruitment of secondary coactivators by SRCs (61, 62). Therefore, the temporal and spatial expression of SRCs may partially determine the transcriptional activation and functions of hLRH-1 in diverse biological processes such as development and metabolism. It will be interesting to examine more SRC-related coactivators on different hLRH-1 regulated promoters.

In contrast to the well-defined molecular events that trigger the ligand-dependent activation of hormone NR, the understanding is still limited in how the transcriptional activities of the constitutively active orphan NRs are regulated. In this study, we demonstrate that SRCs interact directly with hLRH-1 in a novel pattern and potentiates its transcriptional activity. Our findings also illustrate the unique features of hLRH-1 responsible for cofactor recruitment.

MATERIALS AND METHODS

Plasmids

PCR amplifications were performed with the high-fidelity Pyrobest polymerase (TaKaRa, Dalian, China). All plasmids constructed with fragments amplified by PCR were verified by sequencing. Detailed sequence information on the primers used for the plasmid construction is available from the authors.

The pENII/CpLuc reporter was made by cloning the enhancer II and the core promoter (ENII/Cp) region of HBV subtype adr1 (15) in the pGL2basic vector (Promega, Madison, WI). Point mutations that eliminate the hLRH-1 binding site in the ENII B1 element (5′-GATCAACtACaGAtCTcGAG-3′, mutations in *lowercase letters*) were introduced by overlapping PCR as described previously (15). The resulting reporter plasmid was designated pENIIm/CpLuc. The CYP7A1 promoter reporter was made by inserting the −911 to 25 region of hCYP7A1 promoter (11) (the transcription start site is designated 1) amplified by PCR into the *Sma*I/*Xho*I sites of pGL2basic. The GAL4-dependent pG5Luc reporter was made by replacing the chloramphenicol acetyltransferase reporter gene in the pG5CAT (CLONTECH, Palo Alto, CA) with the luciferase gene.

The complete and partial AF2-deleted (aa 1–481) hLRH-1 cDNA (15) were cloned in the pcDNA3 vector (Invitrogen Life Technologies, Carlsbad, CA), respectively, resulting in pcDNA3-hLRH-1 and pAF2-del. After digestion with *Eco*RI and *Xba*I, the complete hLRH-1 cDNA was released from the pcDNA3-hLRH-1 and inserted in the pVP16 vector (CLONTECH) to get pVP16-hLRH-1.

5′-Deletions of the hinge region and the proximal LBD of hLRH-1 were amplified and cloned in the pM vector (CLONTECH), in frame to the GAL4-DBD. The resulting constructs represented fragments aa 141–495, aa 186–495, aa 219–495, aa 228–495, aa 236–495, aa 244–495, aa 256–495, aa 259–495, aa 262–495, aa 325–495, and aa 141–481 of hLRH-1, respectively.

Human SRC-1 cDNA cloned in the pCR3.1 vector (pCR3.1-hSRC-1α) was kindly provided by Dr. M. J. Tsai (Dallas, TX). Original expression plasmids of hTIF2 (TIF2/pSG5) and human ACTR (pCMX-ACTR) were generous gifts from Dr. P. Chambon (Strasburg, France) and Dr. R. M. Evans (La Jolla, CA), respectively. The full-length SRC-1 cDNA was amplified by PCR. After digestion with *Xba*I, it was subcloned downstream from the VP16 activation domain in the blunted *Eco*RI and *Xba*I sites of the pVP16 vector to generate pVP16-SRC-1. Fragments of SRC-1 were also cloned in the pVP16 vector. The resulting constructs represented fragments aa 1–568, aa 568–780, aa 780-1029, aa 1029–1255, aa 1255–

1441, aa 1321–1441, and aa 1029–1441 of SRC-1, respectively. C-terminal fragments of TIF2 and ACTR cDNAs were also inserted in the pVP16 vector. The resulting constructs represented aa 1165–1464 of TIF2 and aa 1142–1412 of ACTR. To make pGAL4-SRC-1, the full-length SRC-1 cDNA in the pVP16-SRC-1 was digested with *Sal*I and *Xba*I and inserted in the same sites of the pM vector. Truncated SRC-1 fragments representing aa 1–1029, aa 1–1255, and aa 1–1321 were amplified by PCR. These fragments were digested with *Kpn*I and *Xba*I and inserted in the same sites of the pCR3.1 vector.

To introduce an internal deletion of aa 1029–1255 into SRC-1, two SRC-1 fragments (aa 1–1028 and aa 1256–1441) were amplified by PCR. After digestion with *Kpn*I and *Bgl*II, *Bgl*II and *Xba*I, respectively, these two fragments were ligated in the *Kpn*I and *Xba*I sites of the pCR3.1 vector. Point mutations that change all three LXXLL motifs to LXXAA in the NID of SRC-1 were introduced by overlapping PCR-mediated mutagenesis. After digestion with *Kpn*I and *Bam*HI, the final fragment replaced the *Kpn*I-*Bam*HI fragment in pCR3.1-hSRC-1α.

The pRC/RSV-mCBP-HA-RK and pCMVβ-p300-CHA expression plasmids were kindly provided by Dr. R. H. Goodman (Portland, OR). The pCMV-mSMRTα-FL expression plasmid was a generous gift from Dr. R. M. Evans (La Jolla, CA).

For expression of GST-hLRH-$1_{186–495}$ fusion protein, the aa 186–495 fragment of hLRH-1 amplified by PCR was digested with *Eco*RI and inserted in the *Sma*I and *Eco*RI sites of the pGEX-3X vector (Amershan Pharmacia Biotech, Uppsala, Sweden). For expression of GST-RARα, the *Sca*I fragment of plasmid pSG5-hRARα (gift from Dr. Z. Chen, Shanghai, China) containing the hinge region and the LBD of hRARα (aa 143–462) was subcloned in the blunted *Eco*RI site of the pGEX-3X vector. Fragments of SRC-1 were also cloned in the pGEX-3X vector, resulting in constructs representing aa 1–568, aa 568–780, aa 780-1029, aa 1029–1255, aa 1255–1441, and aa 1321–1441 of SRC-1, respectively. Fragments of TIF2 (aa 577–796) and ACTR (aa 562–783), which contain the NID of TIF2 or ACTR, respectively, were also cloned in the pGEX-3X vector.

Oligonucleotide-Directed Mutagenesis

Using the pcDNA3-hLRH-1 as the template, point mutations were introduced into the hinge region and helix 1 with GeneEditor *In Vitro* Site-Directed Mutagenesis System (Promega) according to the manufacturer's protocol. All mutations were confirmed by sequencing. The after oligonucleotides were used in the mutagenesis (mutations in *lowercase letters*). TSS_{251}AAA, 5′-TGGATAGTTACCAGgCcgcagCTCCAGCAAGCATC-3′; IL_{260}AA, 5′-CCACATCTGgcAgctAA CTTTTGAAG-3′; E_{261}G, 5′-CTGATACTGGgACTTTTGAAG-3′; LL_{263}AA, 5′-CATCTGATACTGGAAgcTgcaAAGTGTGAGCCAG-3′; and H1_del, 5′-AGCTCTCCAGCAAGCATCCCACATCTG AAGTGTGAGCCAGATGAGCCTCAAGTCCAGG-3′.

Transfection and Luciferase Assays

Huh7, HeLa, and COS cells were grown in DMEM supplemented with 10% fetal calf serum at 37 C and 5% CO_2. Cells were seeded in 35-m dishes at a density of 2.5×10^5 cells per dish and grown for 24 h. One to 4 h before transfection, medium was refreshed. Transient transfections were carried out with the calcium-phosphate precipitation method as previously described (15). Three micrograms of total DNA were used for each transfection, which included 0.5 μg of the pCMV-*lac*Z (Promega) as an internal control to monitor cell viability and to normalize transfection efficiencies among different transfections. When necessary, appropriate amount of the empty vectors (pM, pcDNA3, pCR3.1, and pVP16) were added to ensure equal quantity of DNA among different transfections. Forty-eight hours post transfection, cells were harvested and lysed in 1× Reporter Lysis Buffer (Promega). Luciferase activities were determined with Luciferase Assay System (Promega). β-Galactosidase activities were measured according to a standard colorimetric method (63). Luciferase activities of different transfections were normalized by β-galactosidase activities. Each transfection was performed in duplicate dishes and repeated at least three times.

Western Blotting

Huh7 cells were seeded in 35-mm dishes at a density of 2.5×10^5 cells per dish and were transfected with appropriate expression plasmids and 0.5 μg of the pCMV-*lac*Z. Forty-eight hours post transfection, cells were harvested. A small proportion of the cells were removed for the measurement of the β-galactosidase activity, which was used to monitor cell viability and to normalize the transfection efficiencies among different transfections. The remaining cells were lysed. To ensure equal loading, the amount of cell lysates for each transfection that would be subjected to 10% Tris-glycine SDS-PAGE was adjusted based on the β-galactosidase activity. After electrophoresis, proteins were transferred onto nitrocellulose membrane (PROTRAN; Schleicher & Shnell GmbH, Dassel, Germany). Immunoblotting was carried out with an anti-GAL4-DBD monoclonal antibody SC-510 (Santa Cruz Biotechnology, Inc., Santa Cruz, CA), followed by a rabbit antimouse Ig/horseradish peroxidase (Dako Corp., Carpinteria, CA) as the secondary antibody. Peroxidase activities were detected by the enhanced chemiluminescence reaction with the Western Blot Luminol Reagent (Santa Cruz Biotechnology, Inc.) according to the manufacturer's instruction.

GST Pull-Down Assay

GST fusion proteins were expressed in *E. coli*. BL21(DE3) cultures by the induction with 0.2 mM isopropyl-β-D-thiogalactoside for 2 h at 37 C. Fusion proteins were purified with glutathione-Sepharose 4B beads according to the manufacturer's instruction (Amersham Pharmacia Biotech). Purified proteins were quantified by comparing the sample lanes with a BSA standard on coomassic-stained SDS-PAGE. SRC-1, TIF2, ACTR, hLRH-1, and hRARα proteins were synthesized *in vitro* with the TNT Quick Coupled Transcription/translation System (Promega) in the presence of ^{35}[S] methionine (Amersham Pharmacia) according to the manufacturer's protocol. Pull-down assays were performed using the purified GST fusion proteins and the appropriate labeled proteins. Briefly, 2 μg of a GST fusion protein bound to glutathione-Sepharose beads was incubated with 10 μl of a labeled protein in the binding buffer containing 200 mM KCl at 4 C for 1.5 h. After extensive washing, the mixture was boiled and resolved in 8% or 10% SDS-PAGE. The gel was fixed and dried. Signals were detected by autoradiography.

RT-PCR

Semiquantitative RT-PCR was performed to determine the relative levels of the CYP7A1 transcript among different transfection assays. Huh7 cells were grown in 60-mm dishes and transfected with expression plasmids using the FuGene 6 reagent according to the manufacturer's instruction (Roche Molecular Biochemicals, Indianapolis, IN). Thirty-six hours post transfection, total RNA was isolated with the TRIzol reagent (Invitrogen Life Technologies). Two micrograms of RNA from each sample were used in the reverse transcription reaction with the Moloney murine leukemia virus reverse transcriptase (Promega). For the PCR, the following primer pair was used to amplify a 416-bp fragment of hCYP7A1 cDNA

(forward: 5′-GCATCATAGCTCTTTACCCAC-3′, reverse: 5′-GGTGTTCTGCAGTCCTGTAAT-3′). Meanwhile, a 145-bp fragment of the housekeeping GAPDH cDNA was also amplified (forward: 5′-CCATGACAACTTTGGTATCGTG-3′, reverse: 5′-GCCAGTAG-AGGCAGGGATGA-3′). PCRs were carried out with the following condition: 94 C 1 min, 50 C 1 min, and 72 C 30 sec for 33 cycles for CYP7A1 and 19 cycles for GAPDH. The amplified products were separated on 2% agarose gels and visualized by ethidium-bromide staining. Band density was calculated using the Totallab gel scanning and quantification software. All RT-PCR assays were repeated at least three times.

Detection of SRCs and hLRH-1 in Huh7 cells was performed with standard RT-PCR using after primers to produce fragments located in the C-terminal region of SRCs and the hinge region of hLRH-1, respectively. (SRC-1 forward: 5′-CGAGGTGCTTTTTCACCTGGC-3′, reverse: 5′-CAT GGAG-CTCCCAGGGCTTA-3′; TIF2 forward: 5′-CCAAATCAACTAA-GACTTCAAC-3′, reverse: 5′-GTTACTGTACATGCTGGTGT-TTG-3′; ACTR forward: 5′-CCTCCGCAACAGTTTCCATATC-3′, reverse: 5′-AGACATGGGCATGGGGTTCAT-3′; hLRH-1 forward: 5′-TCCAAAGGCCTACCTC TGAAC-3′, reverse: 5′-AACTATCCATATATGAATAGC-3′). PCRs were carried out with the following condition: 94 C 45 sec, 54 C 45 sec, and 72 C 50 sec for 30 cycles. The amplified products were separated on 1% agarose gel and visualized by ethidium-bromide staining.

Homology Modeling

The LBD of hLRH-1 shares 87% sequence identity and is homologous in function with mLRH-1 LBD. To understand the molecular basis of hLRH-1 transcriptional activity and the potential functional roles of the hinge region and the LBD in the mechanism of transcriptional activation, we built a three-dimensional model of hLRH-1 LBD based on the crystal structure of mLRH-1 LBD (Protein Data Bank entry 1PK5) (41). Sequence alignment between the LBDs from mouse and hLRH-1 was performed using the program CLUSTAL-W (64). The initial model was obtained using the homology-modeling program MODELLER (65). The less conserved regions and buried side chains were manually oriented to have favorable interactions with each other. Models of SRC-1 and SMRT structural segments were docked based on the structures of PPARγ, RXR, and RAR-related orphan receptor in their complexes with SRC-1 and SMRT peptides. The corresponding structures of these complexes were superimposed onto the structural model of hLRH-1 LBD based on the structural alignment of the sandwich framework of nuclear receptors. Molecular dynamics simulation of hLRH-1 LBD model was performed using the program GROMACS (66, 67) in water bath according to the standard procedures of molecular simulations.

Acknowledgments

The authors are grateful to Drs. Ming-Jer Tsai (Baylor College of Medicine, Houston, TX), Richard H. Goodman (OR Health and Science University, Portland, OR), Ronald M. Evans (The Scripps Research Institute, La Jolla, CA), Pierre Chambon (Institut de Genetique et de Biologie Moleculaire et Cellulaire, Illkirch, France), and Zhu Chen (Ruijin Hospital, Shanghai, China) for the original expression plasmids of cofactors in this study, and Dr. Boliang Li (Institute of Biochemistry and Cell Biology, Shanghai, China) for helpful discussion.

Received September 1, 2003. Accepted May 3, 2004.

Address all correspondence and requests for reprints to: Yuan Wang or You-Hua Xie or Jian-Ping Ding, Institute of Biochemistry and Cell Biology, 320 Yueyang Road, Shanghai 200031, China. E-mail:wangy@sibs.ac.cn (Y.W.), yhxie@sibs.ac.cn (Y.-H.X.), jpding@sibs.ac.cn (J.-P.D.).

Current address for M.L.: Institut de Genetique et de Biologie Moleculaire et Cellulaire, 1 rue Laurent Fries, BP 10142, 67404 Illkirch Cedex, France.

This work was supported by the National Natural Science Foundation of China (30100088, 30393112, 30125011, and 30170223), High Technology R&D Project (2001AA221261, 2002BA711A13) from Ministry of Science and Technology, and Innovation Program of Chinese Academy of Sciences (KSCX2-SW-208, KSCX1-SW-17). Y.-H.X. is supported by the Qi Ming Xin Program (01QA14046) from Shanghai Science and Technology Committee, and M.L. by a fellowship from CAS for outstanding Ph.D students.

REFERENCES

1. A unified nomenclature system for the nuclear receptor superfamily. 1999 Cell 97:161–163
2. Ueda H, Sun GC, Murata T, Hirose S 1992 A novel DNA-binding motif abuts the zinc finger domain of insect nuclear hormone receptor FTZ-F1 and mouse embryonal long terminal repeat-binding protein. Mol Cell Biol 12: 5667–5672
3. Crawford PA, Sadovsky Y, Milbrandt J 1997 Nuclear receptor steroidogenic factor 1 directs embryonic stem cells toward the steroidogenic lineage. Mol Cell Biol 17: 3997–4006
4. Hanley NA, Ball SG, Clement-Jones M, Hagan DM, Strachan T, Lindsay S, Robson S, Ostrer H, Parker KL, Wilson DI 1999 Expression of steroidogenic factor 1 and Wilms' tumor 1 during early human gonadal development and sex determination. Mech Dev 87:175–180
5. Rausa FM, Galarneau L, Belanger L, Costa RH 1999 The nuclear receptor fetoprotein transcription factor is coexpressed with its target gene HNF-3β in the developing murine liver, intestine and pancreas. Mech Dev 89: 185–188
6. Falender AE, Lanz R, Malenfant D, Belanger L, Richards JS 2003 Differential expression of steroidogenic factor-1 and FTF/LRH-1 in the rodent ovary. Endocrinology 144: 3598–3610
7. Wang ZN, Bassett M, Rainey WE 2001 Liver receptor homologue-1 is expressed in the adrenal and can regulate transcription of 11β-hydroxylase. J Mol Endocrinol 27:255–258
8. Clyne CD, Speed CJ, Zhou J, Simpson ER 2002 Liver receptor homologue-1 (LRH-1) regulates expression of aromatase in preadipocytes. J Biol Chem 277: 20591–20597
9. Goodwin B, Jones SA, Price RR, Watson MA, McKee DD, Moore LB, Galardi C, Wilson JG, Lewis MC, Roth ME, Maloney PR, Willson TM, Kliewer SA 2000 A regulatory cascade of the nuclear receptors FXR, SHP-1, and LRH-1 represses bile acid biosynthesis. Mol Cell 6:517–526
10. Lu TT, Makishima M, Repa JJ, Schoonjans K, Kerr TA, Auwerx J, Mangelsdorf DJ 2000 Molecular basis for feedback regulation of bile acid synthesis by nuclear receptors. Mol Cell 6:507–515
11. Nitta M, Ku S, Brown C, Okamoto AY, Shan B 1999 CPF: an orphan nuclear receptor that regulates liver-specific expression of the human cholesterol 7α-hydroxylase gene. Proc Natl Acad Sci USA 96:6660–6665
12. Luo Y, Liang CP, Tall AR 2001 The orphan nuclear receptor LRH-1 potentiates the sterol-mediated induction of the human CETP gene by liver X receptor. J Biol Chem 276:24767–24773
13. Schoonjans K, Annicotte JS, Huby T, Botrugno OA, Fayard E, Ueda Y, Chapman J, Auwerx J 2002 Liver recep-

tor homologue 1 controls the expression of the scavenger receptor class B type I. EMBO Rep 3:1181–1187
14. Pare JF, Roy S, Galarneau L, Belanger L 2001 The mouse fetoprotein transcription factor (FTF) gene promoter is regulated by three GATA elements with tandem E box and Nkx motifs, and FTF in turn activates the Hnf3β, Hnf4α, and Hnf1α gene promoters. J Biol Chem 276: 13136–13144
15. Li M, Xie YH, Kong YY, Wu X, Zhu L, Wang Y 1998 Cloning and characterization of a novel human hepatocyte transcription factor, hB1F, which binds and activates enhancer II of hepatitis B virus. J Biol Chem 273: 29022–29031
16. Xie Y, Li M, Wang Y, Hofschneider PH, Weiss L 2001 Site-specific mutation of the hepatitis B virus enhancer II B1 element: effect on virus transcription and replication. J Gen Virol 82:531–535
17. Xu L, Glass CK, Rosenfeld MG 1999 Coactivator and corepressor complexes in nuclear receptor function. Curr Opin Genet Dev 9:140–147
18. Liu D, Chandy M, Lee SK, Le Drean Y, Ando H, Xiong F, Woon Lee J, Hew CL 2000 A zebrafish ftz-F1 (*Fushi tarazu* factor 1) homologue requires multiple subdomains in the D and E regions for its transcriptional activity. J Biol Chem 275:16758–16766
19. Crawford PA, Dorn C, Sadovsky Y, Milbrandt J 1998 Nuclear receptor DAX-1 recruits nuclear receptor corepressor N-CoR to steroidogenic factor 1. Mol Cell Biol 18:2949–2956
20. Monte D, DeWitte F, Hum DW 1998 Regulation of the human P450scc gene by steroidogenic factor 1 is mediated by CBP/p300. J Biol Chem 273:4585–4591
21. Gizard F, Lavallee B, DeWitte F, Teissier E, Staels B, Hum DW 2002 The transcriptional regulating protein of 132 kDa (TReP-132) enhances P450scc gene transcription through interaction with steroidogenic factor-1 in human adrenal cells. J Biol Chem 277:39144–39155
22. Ou Q, Mouillet JF, Yan X, Dorn C, Crawford PA, Sadovsky Y 2001 The DEAD box protein DP103 is a regulator of steroidogenic factor-1. Mol Endocrinol 15:69–79
23. Hammer GD, Krylova I, Zhang Y, Darimont BD, Simpson K, Weigel NL, Ingraham HA 1999 Phosphorylation of the nuclear receptor SF-1 modulates cofactor recruitment: integration of hormone signaling in reproduction and stress. Mol Cell 3:521–526
24. Onate SA, Tsai SY, Tsai MJ, O'Malley BW 1995 Sequence and characterization of a coactivator for the steroid hormone receptor superfamily. Science 270: 1354–1357
25. Takeshita A, Yen PM, Misiti S, Cardona GR, Liu Y, Chin WW 1996 Molecular cloning and properties of a full-length putative thyroid hormone receptor coactivator. Endocrinology 137:3594–3597
26. Kamei Y, Xu L, Heinzel T, Torchia J, Kurokawa R, Gloss B, Lin SC, Heyman RA, Rose DW, Glass CK, Rosenfeld MG 1996 A CBP integrator complex mediates transcriptional activation and AP-1 inhibition by nuclear receptors. Cell 85:403–414
27. Hong H, Kohli K, Trivedi A, Johnson DL, Stallcup MR 1996 GRIP1, a novel mouse protein that serves as a transcriptional coactivator in yeast for the hormone binding domains of steroid receptors. Proc Natl Acad Sci USA 93:4948–4952
28. Voegel JJ, Heine MJ, Zechel C, Chambon P, Gronemeyer H 1996 TIF2, a 160 kDa transcriptional mediator for the ligand-dependent activation function AF-2 of nuclear receptors. EMBO J 15:3667–3675
29. Torchia J, Rose DW, Inostroza J, Kamei Y, Westin S, Glass CK, Rosenfeld MG 1997 The transcriptional coactivator p/CIP binds CBP and mediates nuclear receptor function. Nature 387:677–684
30. Anzick SL, Kononen J, Walker RL, Azorsa DO, Tanner MM, Guan XY, Sauter G, Kallioniemi OP, Trent JM, Meltzer PS 1997 AIB1, a steroid receptor coactivator amplified in breast and ovarian cancer. Science 277:965–968
31. Li H, Gomes PJ, Chen JD 1997 RAC3, a steroid/nuclear receptor-associated coactivator that is related to SRC-1 and TIF2. Proc Natl Acad Sci USA 94:8479–8484
32. Chen H, Lin RJ, Schiltz RL, Chakravarti D, Nash A, Nagy L, Privalsky ML, Nakatani Y, Evans RM 1997 Nuclear receptor coactivator ACTR is a novel histone acetyltransferase and forms a multimeric activation complex with P/CAF and CBP/p300. Cell 90:569–580
33. Takeshita A, Cardona GR, Koibuchi N, Suen CS, Chin WW 1997 TRAM-1, A novel 160-kDa thyroid hormone receptor activator molecule, exhibits distinct properties from steroid receptor coactivator-1. J Biol Chem 272: 27629–27634
34. Suen CS, Berrodin TJ, Mastroeni R, Cheskis BJ, Lyttle CR, Frail DE 1998 A transcriptional coactivator, steroid receptor coactivator-3, selectively augments steroid receptor transcriptional activity. J Biol Chem 273: 27645–27653
35. Voegel JJ, Heine MJ, Tini M, Vivat V, Chambon P, Gronemeyer H 1998 The coactivator TIF2 contains three nuclear receptor-binding motifs and mediates transactivation through CBP binding-dependent and -independent pathways. EMBO J 17:507–519
36. Li J, O'Malley BW, Wong J 2000 p300 Requires its histone acetyltransferase activity and SRC-1 interaction domain to facilitate thyroid hormone receptor activation in chromatin. Mol Cell Biol 20:2031–2042
37. Chen D, Ma H, Hong H, Koh SS, Huang SM, Schurter BT, Aswad DW, Stallcup MR 1999 Regulation of transcription by a protein methyltransferase. Science 284:2174–2177
38. Koh SS, Chen D, Lee YH, Stallcup MR 2001 Synergistic enhancement of nuclear receptor function by p160 coactivators and two coactivators with protein methyltransferase activities. J Biol Chem 276:1089–1098
39. Crawford PA, Polish JA, Ganpule G, Sadovsky Y 1997 The activation function-2 hexamer of steroidogenic factor-1 is required, but not sufficient for potentiation by SRC-1. Mol Endocrinol 11:1626–1635
40. Ito M, Yu RN, Jameson JL 1998 Steroidogenic factor-1 contains a carboxy-terminal transcriptional activation domain that interacts with steroid receptor coactivator-1. Mol Endocrinol 12:290–301
41. Sablin EP, Krylova IN, Fletterick RJ, Ingraham HA 2003 Structural basis for ligand-independent activation of the orphan nuclear receptor LRH-1. Mol Cell 11:1575–1585
42. Wagner RL, Apriletti JW, McGrath ME, West BL, Baxter JD, Fletterick RJ 1995 A structural role for hormone in the thyroid hormone receptor. Nature 378:690–697
43. Ishida H, Ueda K, Ohkawa K, Kanazawa Y, Hosui A, Nakanishi F, Mita E, Kasahara A, Sasaki Y, Hori M, Hayashi N 2000 Identification of multiple transcription factors, HLF, FTF, and E4BP4, controlling hepatitis B virus enhancer II. J Virol 74:1241–1251
44. Ma H, Hong H, Huang SM, Irvine RA, Webb P, Kushner PJ, Coetzee GA, Stallcup MR 1999 Multiple signal input and output domains of the 160-kilodalton nuclear receptor coactivator proteins. Mol Cell Biol 19:6164–6173
45. Heery DM, Kalkhoven E, Hoare S, Parker MG 1997 A signature motif in transcriptional co-activators mediates binding to nuclear receptors. Nature 387:733–736
46. Xu J, Li Q 2003 Review of the *in vivo* functions of the p160 steroid receptor coactivator family. Mol Endocrinol 17:1681–1692
47. Li H, Chen JD 1998 The receptor-associated coactivator 3 activates transcription through CREB-binding protein recruitment and autoregulation. J Biol Chem 273: 5948–5954
48. Misiti S, Schomburg L, Yen PM, Chin WW 1998 Expression and hormonal regulation of coactivator and corepressor genes. Endocrinology 139:2493–2500

49. Xu J, Qiu Y, DeMayo FJ, Tsai SY, Tsai MJ, O'Malley BW 1998 Partial hormone resistance in mice with disruption of the steroid receptor coactivator-1 (SRC-1) gene. Science 279:1922–1925
50. Nishihara E, Yoshida-Komiya H, Chan CS, Liao L, Davis RL, O'Malley BW, Xu J 2003 SRC-1 null mice exhibit moderate motor dysfunction and delayed development of cerebellar Purkinje cells. J Neurosci 23:213–222
51. Sheppard HM, Harries JC, Hussain S, Bevan C, Heery DM 2001 Analysis of the steroid receptor coactivator 1 (SRC1)-CREB binding protein interaction interface and its importance for the function of SRC1. Mol Cell Biol 21:39–50
52. Desclozeaux M, Krylova IN, Horn F, Fletterick RJ, Ingraham HA 2002 Phosphorylation and intramolecular stabilization of the ligand binding domain in the nuclear receptor steroidogenic factor 1. Mol Cell Biol 22: 7193–7203
53. Lee YK, Moore DD 2002 Dual mechanisms for repression of the monomeric orphan receptor liver receptor homologous protein-1 by the orphan small heterodimer partner. J Biol Chem 277:2463–2467
54. Bevan CL, Hoare S, Claessens F, Heery DM, Parker MG 1999 The AF1 and AF2 domains of the androgen receptor interact with distinct regions of SRC1. Mol Cell Biol 19:8383–8392
55. Christiaens V, Bevan CL, Callewaert L, Haelens A, Verrijdt G, Rombauts W, Claessens F 2002 Characterization of the two coactivator-interacting surfaces of the androgen receptor and their relative role in transcriptional control. J Biol Chem 277:49230–49237
56. Darimont BD, Wagner RL, Apriletti JW, Stallcup MR, Kushner PJ, Baxter JD, Fletterick RJ, Yamamoto KR 1998 Structure and specificity of nuclear receptor-coactivator interactions. Genes Dev 12:3343–3356
57. Li X, Wong J, Tsai SY, Tsai MJ, O'Malley BW 2003 Progesterone and glucocorticoid receptors recruit distinct coactivator complexes and promote distinct patterns of local chromatin modification. Mol Cell Biol 23: 3763–3773
58. Gehin M, Mark M, Dennefeld C, Dierich A, Gronemeyer H, Chambon P 2002 The function of TIF2/GRIP1 in mouse reproduction is distinct from those of SRC-1 and p/CIP. Mol Cell Biol 22:5923–5937
59. Xu J, Liao L, Ning G, Yoshida-Komiya H, Deng C, O'Malley BW 2000 The steroid receptor coactivator SRC-3 (p/CIP/RAC3/AIB1/ACTR/TRAM-1) is required for normal growth, puberty, female reproductive function, and mammary gland development. Proc Natl Acad Sci USA 97:6379–6384
60. Apostolakis EM, Ramamurphy M, Zhou D, Onate S, O'Malley BW 2002 Acute disruption of select steroid receptor coactivators prevents reproductive behavior in rats and unmasks genetic adaptation in knockout mice. Mol Endocrinol 16:1511–1523
61. Puigserver P, Adelmant G, Wu Z, Fan M, Xu J, O'Malley B, Spiegelman BM 1999 Activation of PPARγ coactivator-1 through transcription factor docking. Science 286: 1368–1371
62. Picard F, Gehin M, Annicotte J, Rocchi S, Champy MF, O'Malley BW, Chambon P, Auwerx J 2002 SRC-1 and TIF2 control energy balance between white and brown adipose tissues. Cell 111:931–941
63. Sambrook J, Fritsch EF, Maniatis T 1989 Molecular cloning. Cold Spring Harbor, NY: Cold Spring Harbor Laboratory
64. Thompson JD, Higgins DG, Gibson TJ 1994 CLUSTAL W: improving the sensitivity of progressive multiple sequence alignment through sequence weighting, position-specific gap penalties and weight matrix choice. Nucleic Acids Res 22:4673–4680
65. Sali A, Potterton L, Yuan F, van Vlijmen H, Karplus M 1995 Evaluation of comparative protein modeling by MODELLER. Proteins 23:318–326
66. Berendsen HJ, van der Spoel D, van Drunen R 1995 GROMACS: a message-passing parallel molecular dynamics implementation. Comp Phys Comm 91:43–56
67. Lindahl E, Hess B, van der Spoel D 2001 GROMACS 3.0: a package for molecular simulation and trajectory analysis. J Mol Mod 7:306–317

***Molecular Endocrinology* is published monthly by The Endocrine Society (http://www.endo-society.org), the foremost professional society serving the endocrine community.**